Quantum Critical Matter and Phase Transitions in Rare-Earths and Actinides

Louk Rademaker*

Kavli Institute for Theoretical Physics, University of California Santa Barbara, California 93106, USA

J. A. Mydosh†

Kamerlingh Onnes Laboratory and Institute-Lorentz, Leiden University, P.O. Box 9504, NL-2300 RA Leiden, The Netherlands

(Dated: November 25, 2015)

In this Chapter we discuss quantum criticality, the notion that properties of a material are governed by the existence of a phase transition at zero temperature. The point where a second-order (continuous) phase transition takes places is known as a quantum critical point (QCP). Materials that exhibit a quantum critical points can be tuned through their quantum phase transition by, for example, pressure, chemical doping or disorder, frustration, and magnetic field. The study of quantum phase transitions (QPT) was initially theoretically driven, showing that high-temperature properties of a material with a QPT are directly influenced by the properties of the QCP itself. We start this Chapter by discussing the predictions of quantum critical and Hertz-Millis theory. Experimentally, we will mainly limit ourselves to f-electron based materials: the rare-earths Li(Ho,Y)F_4, Ce(Cu,Au)$_6$, $YbRh_2Si_2$, the Cerium series Ce(Co, Rh; Ir)In_5 and one actinide based material, URu_2Si_2. These 'heavy fermion' metals ($4f$ or $5f$) represent prototype materials of quantum critical matter, and we will critically review their experimental signatures and their evolving theoretical descriptions. We conclude with other manifestations of quantum phase transitions beyond the rare-earths and actinides.

PACS numbers: 71.27.+a, 74.70.Tx; 75.30.Mb

Contents

*Electronic address: louk.rademaker@gmail.com
†Electronic address: mydosh@physics.leidenuniv.nl

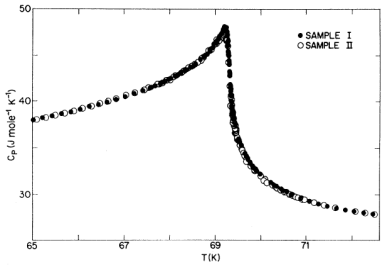

FIG. 1. Specific heat of EuO (samples I and II) as a function of T.

FIG. 1 The specific heat around the ferromagnetic transition in EuO, at T_c = 69K. The critical exponent is $\alpha \approx$ -0.044, indicating a near logarithmic divergence. According to Kornblit and Ahlers (1975).

I. INTRODUCTION

Many compounds based on rare earth and actinide elements, such as $Ce(Cu,Au)_6$ and $YbRh_2Si_2$, display unusual electronic and magnetic properties. "Unusual" is used in a strong sense such that standard Fermi liquid theory is not applicable, and a proper theoretical description is still lacking.

However, driven by a theoretical effort it has been suggested that many properties can be understood within the framework of a "quantum phase transition": a second-order phase transition from a magnetically ordered state at zero temperature to a new quantum phase. Such a zero temperature phase transition leads to a dramatic change of the electronic properties at finite, nonzero temperatures.

There are many good reviews on quantum phase transitions, for example Gegenwart et al. (2008); Pfleiderer (2009); Sachdev (2008); von Löhneysen et al. (2007). Unlike those reviews we will not be complete in the enumeration of all measured properties of all possible quantum critical compounds. Instead, we want to provide a critical view on quantum phase transitions in certain prototype rare-earth and actinide-based compounds.

The concept of quantum criticality, which we will discuss in-depth in Section II, has lead to a surge of novel concepts, most importantly of them is scaling. Scaling suggests that many measurable quantities such as the specific heat coefficient, the thermal expansion, magnetic susceptibility, etc, have simple power-law behavior as a function of temperature, pressure or magnetic field. Indeed, some materials are fully described the scaling laws as derived by the theory of Hertz, Millis and Moriya. However, it was soon found that many materials - such as $Ce(Cu,Au)_6$ and $YbRh_2Si_2$ - not only violate Fermi liquid theory, but also Hertz-Millis theory.

After presenting these compounds, we elaborate in Section III on the shortcomings of Hertz-Millis (HM) theory and recent attempts to better theories. In line with our philosophy, we will review those theories critically: unfortunately, many of them are either based on unquantifiable assumptions or lack a microscopic derivation.

Nonetheless, the conceptual power of quantum criticality still stands, and the novel non-Fermi liquid materials Ce-115 and URu_2Si_2 are looked at through quantum critical glasses. By discussing difficulties associated with 'hidden' quantum critical points, disorder and material stability we aim to show in Section IV the challenges and opportunities associated with using concepts from quantum phase transitions. Section V lists other forms of quantum matter beyond the rare earths and actinides.

II. HISTORICAL BACKGROUND

A. Classical Continuous Phase Transitions

This Chapter deals with phase transitions of a special kind, namely quantum critical points. Before delving into that topic, we need to review some general properties of phase transitions. Most phase transitions we encounter in daily life, like the liquid-gas or the freezing transition, are of the first order kind. First order transitions are characterized by a rapid discontinuous change of the material properties, and release (or absorb) latent heat.

Second order or continuous phase transitions (CPT) are more subtle. No latent heat is involved, but the specific heat still displays non-analytic behavior in the form of a divergence or a kink. In terms of the *reduced temperature*

$t = \frac{T-T_c}{T_c}$, where T_c is the transition temperature itself, the specific heat behaves as a power-law,

$$C_v \sim |t|^{-\alpha}, \tag{1}$$

where α is the *specific heat critical exponent*. A typical example is shown in Fig. 1, which shows the specific heat around the ferromagnetic transition in EuO.

Any phase transition can be described by an *order parameter*, a quantity that is zero in one phase and nonzero in the other. In a ferromagnet this would be the net magnetization, in an antiferromagnet the staggered magnetization, in a superconductor the superfluid density. Unlike a first order transition, where the order parameter jumps discontinuously, the order parameter m at a CPT goes to zero in a power-law fashion,

$$m \sim (-t)^{\beta}, \tag{2}$$

for $t < 0$, and where β is the *order parameter critical exponent*.

The key element of a CPT is that at the transition, fluctuations *at all length scales* play an important role. Away from the critical point, fluctuations of the order parameter have a typical finite *correlation length* ξ. This correlation length diverges close to the critical point,

$$\xi \sim |t|^{-\nu} \tag{3}$$

with ν the *correlation length critical exponent*. Similarly, the susceptibility associated with the order (eg. the magnetic susceptibility $\chi = \frac{\partial M}{\partial H}$ for a ferromagnet) also diverges at the critical point, which defines the *susceptibility exponent*

$$\chi \sim |t|^{-\gamma}. \tag{4}$$

A list of most commonly used exponents is shown in Table I. All of those exponents are accessible in experiments, for example Table III in Kornblit and Ahlers (1975) includes all the critical exponents for the ferromagnetic transition in EuO.

Because fluctuations at all length-scales become equally important, many of the microscopic details of the system become irrelevant. As a result, important physical quantities can be expressed as scaling functions of the diverging correlation length and other macroscopic parameters. For example, for many CPTs the free energy density is just a function of the correlation length itself, $f \sim \xi^{-d}$, where d is the dimensionality of the system. If this is the case, it follows that the specific heat exponent is related to the correlation length exponent by the *hyperscaling relation* $2 - \alpha = \nu d$. Other such scaling relations, that can be directly derived from the notion of physics-at-all-length-scales, are $2 - \alpha = 2\beta + \gamma$, $2 - \alpha = \beta(\delta + 1)$ and Fishers relation $\gamma = (2 - \eta)\nu$.

These scaling relations highly constrain the possible values the critical exponents can take. In fact, only the symmetry of the order parameter and the dimensionality of the system are relevant in order to determine the critical exponents of a transition. This is the concept of *universality*: every CPT belongs to a universality class (Ising, XY, Heisenberg, etc.) of transitions with the same critical exponents, even though the underlying microscopic physics can be completely different. The beautiful principle of universality has made the study of CPTs among the most popular in modern science.

As early as 1971 Stanley published the first book on phase transitions and critical phenomena(Stanley, 1971), followed by Ma (1976), Goldenfeld (1992), Yeomans (1992) and Herbut (2010). Into the 2000's a series of multivolume monographs have appeared, edited by Domb and Lebowitz (2001). At the present CPTs are well understood, from both a experimental as well as theoretical point of view(Nishimori and Ortiz, 2010). Whenever a new magnetic material is fabricated, one just needs to verify if a CPT occurs and check its universality class. Once that is known, all is known about that particular phase transition.

B. Quantum critical theory

A quantum phase transition is a second order phase transition that occurs at zero temperature, as a function of pressure, magnetic field or any tuning parameter g other than temperature. A standard way of obtaining such a transition is by suppressing the critical temperature of an ordered state - such as a ferromagnet or antiferromagnet - to zero temperature by for example pressure. When the pressure exceeds the critical pressure, a quantum disordered regime appears.

Exactly at the critical value of the tuning parameter $g = g_c$, the system develops many unconventional properties. The relevance of quantum phase transitions is that for nonzero temperatures close to the critical value g_c the system is still dominated by quantum critical excitations. Thus can arise unconventional specific heat, resistivity, magnetic

TABLE I The definition of several critical exponents for a magnetic material exhibiting a continuous phase transition. The first column indicates the physical observable, the second the exponent. The third column indicates how the observable scales near a finite temperature phase transition as a function of the reduced temperature $t = \frac{T-T_c}{T_c}$. The fourth column shows how the observable scales near a quantum phase transition, as a function of the control parameter $g - g_c$.

Quantity	Exponent	Finite Temperature	Quantum Phase Transition
order parameter	β	$m \sim (-t)^\beta$	$m \sim (g-g_c)^\beta$
specific heat	α	$C \sim \lvert t\rvert^{-\alpha}$	—
susceptibility	γ	$\chi \sim \lvert t\rvert^{-\gamma}$	$\chi \sim \lvert g-g_c\rvert^{-\gamma}$
critical isotherm (at $t=0$ or $g=g_c$)	δ	$B \sim \lvert m\rvert^\delta$	$B \sim \lvert m\rvert^\delta$
correlation length	ν	$\xi \sim \lvert t\rvert^{-\nu}$	$\xi \sim \lvert g-g_c\rvert^{-\nu}$
correlation function (at $t=0$ or $g=g_c$)	η	$G(r) \sim \lvert r\rvert^{-d+2-\eta}$	$G(r) \sim \lvert r\rvert^{-d+2-\eta}$
dynamics	z	—	$\xi_\tau \sim \xi^z$

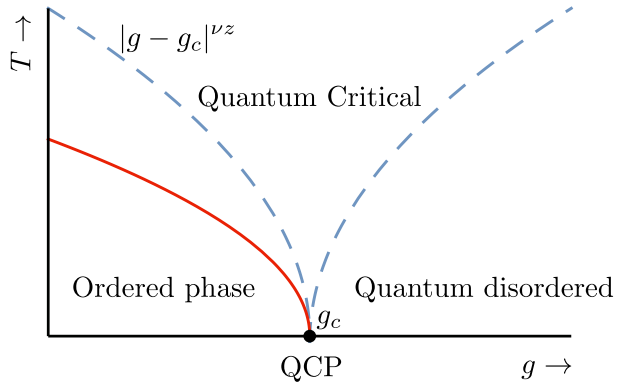

FIG. 2 The typical phase diagram of a quantum phase transition. On the horizontal axis we put a tuning parameter g, which can be pressure, magnetic field or particle density; the vertical axis represents temperature. The high g regime to the right represents the 'quantum disordered' phase: a paramagnet or just a regular Fermi liquid. At low g there is an ordered phase, for example a (anti)ferromagnet. The quantum critical point resides exactly at $T = 0$ where the system goes from the ordered to the disordered phase. At this critical value of $g = g_c$, the nonzero temperature regime is denoted as 'quantum critical'. In this part of the phase diagram many properties such as the specific heat or the resistivity are unconventional due to the vicinity of the quantum critical point. Such unconventional behavior is usually referred to as 'Non-Fermi liquid' behavior.

susceptibility, and so on. This 'quantum critical regime', as shown in the typical phase diagram of Fig. 2, is thought to be the key towards understanding many abnormal properties of materials.

In this section we first provide the traditional theory of how such a quantum critical regime appears. As for all phase transitions, the key lies in the concept of scaling functions and the corresponding exponents close to the transition. In fact, there is an intricate link between quantum phase transitions and thermal phase transitions, which becomes clear by considering the example of the Ising model.

Critical exponents for any given model can be computed using the methods of statistical physics. The starting point is to define the microscopic Hamiltonian H relevant for the system under study. For the *Ising model*, a model of interacting spins that can describe (anti)ferromagnetic phase transitions, the Hamiltonian is

$$H = -J \sum_{\langle ij \rangle} S_i^z S_j^z, \tag{5}$$

where S_i^z is the z-component of a classical spin at a lattice site i. For $J > 0$ this model has a ferromagnetic ground state, and we therefore expect that below some temperature the system develops spontaneous magnetization.

The Ising model is classical, so that the partition function $\mathcal{Z} = \sum_n e^{-\beta E_n}$, where the sum runs over all possible spin states with energy E_n. Any macroscopic quantities that we are interested in, such as magnetization or specific heat, can be derived from the free energy $\mathcal{F} = -k_B T \log \mathcal{Z}$. In some cases the partition function and hence the free energy can be computed exactly, in most cases, however, we need to resort to an approximation scheme.

The most successful theory is Landau mean field theory: here we assume that spins interact only with the average field of all other spins, given by $m(x)$. A free energy functional can then be written as a function of the magnetization

$m(x)$ and temperature T. In general, for a d-dimensional system, we have

$$\mathcal{F}(m,T) = \int d^d x \left(c(\nabla m(x))^2 + a_2(T) m(x)^2 + a_4 m(x)^4 + \ldots \right) \tag{6}$$

where a_2, a_4 and c are some parameters. For a continuous phase transition, Landau showed, we must have $a_2 \sim t$ with t the reduced temperature, a_4 and c are positive definite. The magnetization can be found by minimizing $\mathcal{F}(m,T)$ with respect to the order parameter $m(x)$.

From just these very general considerations, we can compute critical exponents. For example, minimizing the free energy with respect to a homogeneous m gives us the order parameter exponent $\beta = 1/2$. The second derivative $C_V = \frac{\partial^2 F}{\partial T^2}$ yields the specific heat exponent $\alpha = 0$. Explicitly writing out the correlation functions for an inhomogeneous order parameter $m(x)$ yields $\nu = 1/2$ and $\eta = 0$. Finally, an external magnetic field can be included by adding $-h \int d^d x m(x)$ to the free energy, which yields $\delta = 3$ and $\gamma = 1$. (See chapter 4 from Yeomans (1992) for more details.)

Mean field theory ignores fluctuations, but with increasing dimensionality of the system these fluctuations become less and less relevant. In fact, the mean field exponents become exact in $d > \frac{2-\alpha}{\nu}$ dimensions. This is called the *upper critical dimension*, so that for example the Ising model in $d > 4$ dimensions is determined by mean field exponents.

We are now in a position to continue towards quantum systems, where the phase transition does not occur as a function of temperature but at zero temperature due to a change in model parameters. Because in a quantum system the Hamiltonian is an operator the partition function is now given by,

$$\mathcal{Z} = \mathrm{Tr} \exp\left(-\beta \hat{H}\right). \tag{7}$$

The Ising model can be extended to a quantum model, known as the *transverse field Ising model*. The properties of this model are described in detail by Sachdev (2011). It is the prime example of a magnetic system exhibiting a quantum phase transition. The Hamiltonian is

$$H_{TFIM} = -Jg \sum_i S_i^x - J \sum_{\langle ij \rangle} S_i^z S_j^z \tag{8}$$

where $J > 0$ is the magnetic exchange coupling between spins, and g is the magnitude of a transversal magnetic field. Now g acts as the tuning parameter that can induce a phase transition between a ferromagnetic phase and a paramagnetic phase. For g$\ll$1 (ferro)magnetic order prevails with two possible ground states,

$$|\psi_0\rangle = \prod_i |\uparrow\rangle_i, \text{ or } \prod_i |\downarrow\rangle_i. \tag{9}$$

Oppositely, for a large transverse field g$\gg$1, the ground state is an uncorrelated ($\langle S_i^z S_j^z \rangle = \delta_{ij}$) paramagnet

$$|\psi_0\rangle = \prod_i |\rightarrow\rangle_i = \prod_i (|\uparrow\rangle_i + |\downarrow\rangle_i)/\sqrt{2}.$$

The paramagnet and the ferromagnet are distinctively different. Therefore, under increase of the transverse field g there will be a quantum phase transition from the ferro- to the paramagnet at $g = g_c$.

Suzuki (1976) discovered that the free energy of the d-dimensional quantum Ising model is equivalent to the $(d+1)$-dimensional classical Ising model. Explicitly, the quantum partition function can be rewritten as a Feynman path integral where the inverse temperature $\beta = 1/k_B T$ acts an extra dimension called imaginary time $\tau \in [0, \beta)$. At zero temperature, the free energy for the d-dimensional quantum Ising model becomes

$$\mathcal{F}(m,g) = \int d^d x d\tau \left\{ c(\partial_\mu m(x,\tau))^2 + a_2(g) m(x,\tau)^2 + a_4 m(x,\tau)^4 + \ldots \right\}, \tag{10}$$

so that the tuning parameter is now g as opposed to T for the classical phase transition.

The parameter $a_2 \sim (g - g_c)$ changes sign when the transverse field is increased. At the transition not only spatial correlation length diverges, also the imaginary time correlations ξ_τ. They are related by the dynamical critical exponent z,

$$\xi_\tau \sim \xi^z. \tag{11}$$

It is easy to see that for the Ising model, the dynamical critical exponent is $z = 1$, since x and τ are treated on the

same footing.

All other critical exponents can be derived from the critical exponents of the $(d+1)$-dimensional classical Ising model. We have $m \sim (g-g_c)^\beta$ for the order parameter, and similar expressions for the susceptibility exponents and the correlation length exponents. All of those are listed in Table I. Note that there is not an analogue of the specific heat exponent at zero temperature.

In conclusion, we note that both classical and quantum field theories are described by a free energy functional that depends on the order parameter. The quantum transverse field Ising model in d dimensions is equivalent to the classical Ising model in $(d+1)$ dimensions. This allows us to find the critical exponents associated by the quantum phase transition in the quantum Ising model from the classical exponents. In Sec. II.D.1 we will discuss $Li(HoY)F_4$, a rare earth material that displays characteristics of a quantum Ising phase transition.

C. Hertz-Millis theories of itinerant magnets

In many rare earth materials the magnetism is not caused by localized spins as described by the Ising model. Instead, it consists of conducting (itinerant) electrons that undergo a spin-density wave transition or a superconducting transition. The theory of quantum phase transitions in the presence of interacting electrons was pioneered by Hertz (1976), Millis (1993) and Moriya (1985).

Their theory starts with interacting electrons, for which one can write down the partition function at inverse temperature β, defined by Eqn. (7). These interacting electrons have an instability towards the formation of some kind of magnetic order. The magnitude of the magnetic order is parametrized by the order parameter field $\Psi(x,\tau)$ where x is the spatial coordinate and τ the imaginary time - the extra dimension as a consequence of quantum physics.

The key assumption in Hertz-Millis theories is that the low-energy physical description of this system can do without referring to electrons. All electronic degrees of freedom can be integrated out and we are left with an effective free energy (also sometimes called 'action') depending on the order parameter field $\Psi(x,\tau)$. For example, for an itinerant ferromagnet this leads to

$$\mathcal{F}[\Psi] \;=\; \frac{1}{2}\sum_{q\omega}\left(r_0 + q^2 + \frac{|\omega|}{q}\right)|\Psi(q,\omega)|^2 + \frac{u_0}{4N\beta}\sum_{q_i\omega_i}\Psi_1\Psi_2\Psi_3\Psi_4\delta\left(\sum q\right)\delta\left(\sum\omega\right) \tag{12}$$

where (q,ω) are momentum and energy, the Fourier transform of (x,τ); r_0 is the tuning parameter that makes the system ferromagnetic or paramagnetic, and u_0 is some effective order parameter interaction. Since this is a low-energy effective field theory, the correct way to study this is through renormalization group theory(Herbut, 2010; Wilson and Kogut, 1974; Yeomans, 1992) - a topic that goes beyond this brief review. Instead, we can infer the most important results from simple scaling arguments.

A scaling argument uses that at the quantum phase transition, physical properties are the same at all length scales. Hence, if we multiply the momenta q and the energies ω with some factor, the action Eqn. (12) should remain invariant. The difference between the scaling of momenta and energies is characterized by the dynamical critical exponent z, recall Eqn. (11). Simple inspection of the ferromagnetic action (12) implies $z=3$. Similarly, for antiferromagnets we find $z=2$.(Hertz, 1976)

The upper critical dimension for this model is no longer 4, as was the case for the classical Ising model, but $4-z$ with z the dynamical critical exponent. This implies that the ferromagnetic quantum phase transition in $d>1$ and the antiferromagnetic QPT in $d>2$ can be described by mean field exponents!

The scaling arguments can be extended to nonzero temperatures. Whenever the inverse temperature β is smaller than the imaginary time correlation length ξ_τ, one expects that quantum critical fluctuations are dominant. This leads to the famous 'quantum critical wedge',

$$T > (g-g_c)^{\nu z}, \tag{13}$$

the temperature regime where the system can be described as 'quantum critical' and standard lore about interacting fermions no longer applies. In this regime a scaling ansatz for the free energy can be formulated,(Zhu et al., 2003)

$$\mathcal{F}(T) \sim \frac{1}{\xi^d \xi_\tau}\widetilde{f}\left(T\xi_\tau\right) \sim |g-g_c|^{(d+z)\nu}\widetilde{f}\left(\frac{T}{|g-g_c|^{\nu z}}\right) \tag{14}$$

from which we can directly infer that the low-temperature specific heat scales as

$$c_V(T, g=g_c) = -T\frac{\partial^2\mathcal{F}}{\partial T^2} \sim T^{d/z}. \tag{15}$$

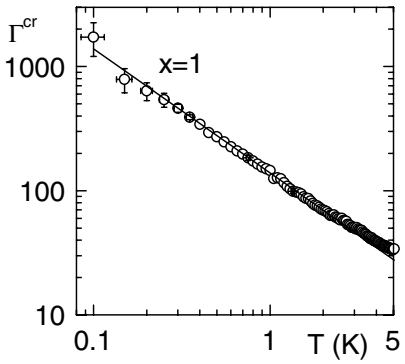

FIG. 3 The critical Grüneisen ratio $\Gamma^{cr} = \alpha^{cr}/c_V^{cr}$ of $CeNi_2Ge_2$, on a log-log plot as a function of temperature at ambient pressure and zero field. The noncritical contributions to the specific heat c_V and the thermal expansion α have been subtracted. The solid line represents $\Gamma \sim 1/T$, consistent with Hertz-Millis theory. From Küchler et al. (2003).

This is notably different from the standard Fermi liquid result of a linear specific heat $c_V(T) \sim \gamma T$ where γ is the Sommerfeld coefficient. That is why the system inside the quantum critical wedge is often referred to as a 'Non-Fermi Liquid' (NFL).

The typical smoking gun for NFL behavior is an unconventional temperature dependence of the resistivity,

$$\rho(T) = \rho_0 + aT^n \tag{16}$$

where $n = 2$ would be for a standard Fermi liquid. Many materials have n deviating from two - for example the linear resistivity measured in $YbRh_2Si_2$(Custers et al., 2003). Within the theoretical framework of Hertz-Millis theory, indeed anomalous exponents were found(Moriya and Takimoto, 1995), for example $\Delta\rho \sim T^{3/2}$ at a $d = 3$ antiferromagnetic quantum critical point. However, this picture fails when the electron scattering is peaked at 'hot spots' on the Fermi surface, that are connected by the antiferromagnetic wavevector $\vec{Q}$. There critical fluctuations lead to a linear T scattering rate, but electrons on the remaining 'cold spots' still follow the standard Fermi liquid lure and the overall resistivity is expected to be $\Delta\rho \sim T^2$ again.(Hlubina and Rice, 1995) Disorder can change this picture again(Rosch, 1999, 2000), which makes resistivity a difficult subject matter.

Not all NFL behavior arises due to quantum criticality. To distinguish between NFL behavior due to disorder(Westerkamp et al., 2009) and actual criticality, the Grüneisen ratio Γ was introduced. For any quantum critical point controlled by pressure, the ratio between the thermal expansion $\alpha = -\frac{1}{V}\frac{\partial S}{\partial p}$ and the specific heat at the critical pressure should diverge(Zhu et al., 2003),

$$\Gamma(T, p = p_c) = \frac{\alpha}{c_V} \sim T^{-1/\nu z}. \tag{17}$$

The standard theory of Hertz-Millis for a three-dimensional antiferromagnetic QPT gives $z = 2$ and the mean field correlation length exponent $\nu = 1/2$, hence the Gruneisen ratio should diverge as $1/T$.

A group of cerium-based compounds does seem to exhibit the critical behavior as predicted by Hertz-Millis theory. Most notable is $CeNi_2Ge_2$: at ambient pressure and zero field this material has a critical specific heat $c_V \sim T^{3/2}$ and a Grüneisen ratio $\Gamma \sim T^{-1}$, consistent with the Hertz-Millis predictions, see Fig. 3.(Küchler et al., 2003) The resistivity is found to be $\Delta\rho(T) \sim T^{3/2}$.(Gegenwart et al., 1999) There only suspicious aspect of this material is that it doesn't have an antiferromagnetic phase. The isostructural compound $CePd_2Si_2$ does become antiferromagnetic, and it has been suggested that the critical behavior of $CeNi_2Ge_2$ is connected to the high-pressure quantum critical point in $CePd_2Si_2$.(Grosche et al., 2000) Consequently, antiferromagnetic order in $CeNi_2Ge_2$ should exist at 'negative' pressures - a challenging concept indeed. Two other related compounds, $CeCu_2Si_2$ and $CeCu_2Ge_2$, seem to have similar Hertz-Millis quantum critical behavior(Stockert et al., 2004) but it appears hard to synthesize these materials consistently.(von Löhneysen et al., 2007)

As mentioned before, the Grüneisen ratio will diverge for *any* quantum critical point, even when it cannot be described by Hertz-Millis theory. For example, in both $CeCu_{6-x}Au_x$ (see section II.D.2) and $YbRh_2Si_2$ (see section II.D.3) the Gruneisen ratio diverges, though with a different exponent than is expected from Hertz-Millis theory.(Küchler et al., 2003, 2004; Tokiwa et al., 2009)

We have so far only considered static properties. Criticality can also be inferred from dynamical properties, such

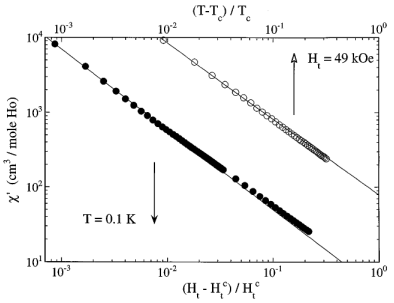

FIG. 4 The divergence of the ac magnetic susceptibility as a function of the reduced critical temperature and $H_\perp$ field. T_c has been defined as the lowest temperature of measurement 0.114K while the extrapolated to T=0 $H_\perp$ is 4.93T. All the susceptibility divergence are mean field like with critical exponent $\gamma = 1$, meaning no difference between the zero field ferromagnetic transition and the field tuned QPT. According to Bitko et al. (1996).

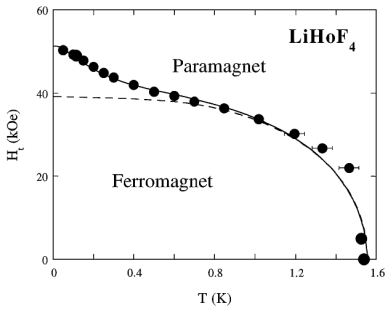

FIG. 5 Experimental phase diagram for $LiHoF_4$ with a ferromagnetic phase up to the Curie temperature, as a function of T_c and applied transverse field $H_\perp$. The dashed line represents the mean-field theory while the solid line and data points include the correction due to the nuclear hyperfine interaction. Here $H_\perp^c$ is 4.93T and the lowest measurement temperature is 0.1K. The divergence of the ac-susceptibility (χ' and χ'') in the given field determines $T_c(H_\perp)$. According to Bitko et al. (1996).

as the dynamical susceptibility $\chi(k,\omega)$. For example, Sachdev (2011) introduced the scaling function

$$\chi(k,\omega) \sim T^{-(2-\eta)/z}\Phi\left(\frac{k}{T^{1/z}}, \frac{\omega}{T}, \frac{\Delta}{T}\right) \tag{18}$$

where Δ is the gap on either side of the transitions, so $\Delta \to 0$ at the transition.

It is important to note that in numerous rare earth materials unconventional superconductivity is found (for a review, see Pfleiderer (2009)). In a superconductor, electrons are bound together into a Cooper pair. Understanding a superconducting phase thus boils down to finding the 'glue', and it has been suggested that quantum critical fluctuations could act as glue.(Mathur et al., 1998; Metlitski et al., 2015; Miyake et al., 1986; Scalapino et al., 1986; She and Zaanen, 2009) The quantum phase transition associated with the disappearance of magnetism is then obscured by a 'superconducting dome'. Whereas the idea is appealing, there are as of yet no clear experimental way to discern whether a quantum critical point truly exists below the dome.

Finally, note that in the spin-density-wave picture presented in this section, the electrons play a secondary role. This means that throughout the transition, all properties of the electrons themselves such as their effective mass or their Fermi surface shape, can only change continuously. (Gegenwart et al., 2008) In Sec. III, we will discuss scenarios inspired by experiments that challenge this notion of electrons as mere bystanders.

D. Experiments: Li(Ho,Y)F_4, Ce(Cu,Au)$_6$ and $YbRh_2Si_2$

1. Li(HoY)F_4

Once the theoretical considerations for quantum criticality in the transverse field Ising model became known, the search began for a real material to display this QPT. The chosen "ideal" compound was pure $LiHoF_4$, a dipolar-coupled insulating ferromagnet with strong Ising anisotropy and small Curie temperature $T_C = 1.53K$. The first

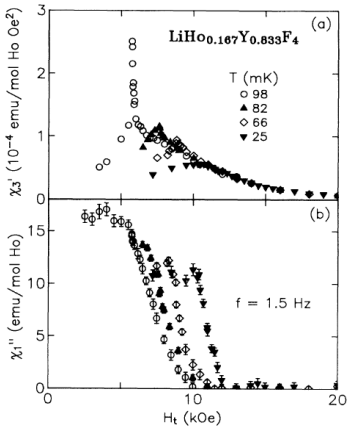

FIG. 6 Upper panel: Non-linear ac-susceptibility as function of H⊥ at various temperatures. Note how the originally sharp classical SG transition is smeared into a broad peak as the QCP is reached. Lower panel: Imaginary part (absorption) of the linear ac-susceptibility as above. Note how the absorption decreases as the $H_\perp$ is scanned though the critical temperature both classical and quantum. This behavior indicates dynamical effects around the transitions at the one frequency (1.5Hz) of measurement. According to Wu et al. (1993).

experiments(Bitko et al., 1996) measured ac-magnetic susceptibility down to 0.05K in $H_\perp$ up to 8T. The results for both the classical ferromagnetic transition and the QPT (at T≈0 with critical field $H_\perp^C = 4.93$T) showed in both cases a mean-field susceptibility divergence, i.e., the susceptibility exponent γ was approximately 1. Figure 4 exhibits the divergences as function of T near $H_\perp^C$ and function of ($H_\perp$ - $H_\perp^C$)/$H_\perp^C$ at constant T, where we see the near linear dependences.

Figure 5 presents the experimental phase diagram (external field $H_\perp$ vs. T) of $LiHoF_4$. The low temperature, high-field deviations from the mean field behavior is attributed to nuclear hyperfine interactions of the holium. Inelastic neutron scattering experiments showed that the expected mode-softening at the QPT was perturbed and discontinued by the hyperfine coupling to the nuclear spins that prevented a detailed study of the QPT (Rønnow et al., 2005, 2007).

Early on, experiments of specific heat in $H_\perp$ were performed that spanned the $H_\perp^C$ (Mennenga et al., 1984). However, the then unknown QCP was not reached in temperature and the results merely confirmed the reduced but smeared out in $H_\perp$ specific heat peak of the ferromagnetic transition with an incipient upturn at the lowest temperature. The hyperfine modification to the QPT discouraged further experiments at the QCP and attention then shifted to the diluted $Li(Ho_xY_{1-x})F_4$ compounds and its putative quantum spin-glass phase transition according to the older work of Wu et al. (1993). However, this left the quantum critical and quantum fluctuation portions of the $LiHoF_4$ phase diagram mostly unexplored.

Even before the interest in the transverse field QPT of Ising $LiHoF_4$ became apparent, the search for a spin glass state in diluted $Li(Y_{1-x}Ho_x)F_4$ was underway via ac-susceptibility (Reich et al., 1986). The initial question posed: can the reduced holmium concentration (e.g., $x = 0.167$) and random dipolar interactions create a canonical Ising spin glass? The efforts are continuing up to the present with the answer still being controversial. Jönsson et al. (2007) claim the absence of a conventional spin-glass transition, based on low temperature SQUID measurements. In contrast Ancona-Torres et al. (2008) using low field, low-frequency nonlinear susceptibility established the spin-glass transition. Other experiments are divided between a canonical spin glass phase (Quilliam et al., 2012), and glassy low-temperature dynamics (Rodriguez et al., 2010).

Regardless of the exact spin-glass state, the behavior of diluted $Li(Y_{1-x}Ho_x)F_4$ in a transverse field $H_\perp$ was studied, motivated by theoretical predictions of Read et al. (1995) and Sachdev (2011). Initially, Wu et al. (1993) investigated the non-linear susceptibility of the $x = 0.167$ compound to low temperatures and high fields, thereby driving the spin glass temperature $T_SG(H_\perp)$ to near zero as shown in Figure 6. As 25mK was approached by varying $H_\perp$, the non-linear susceptibility became broadened with no sign of the expected QCP divergence and unconventional frequency effects (Kopeć, 1997). Wu et al. (1993) then suggested the disagreements with theory were the result of a first-order quantum spin-glass transition. More recent measurements (Tabei et al., 2006) attribute this lack of QPT behavior to the induced random field Ising model thereby rendering the quantum criticality inaccessible. This conclusion was confirmed by Ancona-Torres et al. (2008) due to the competing effects of quantum entanglement and random fields. Schechter (2008) has demonstrated that a proper treatment of $LiHo_xY_{1-x}F_4$ in a transverse field is the random field-Ising model, not the canonical QPT description introduced in Section II.B. Additional attempts at finding an Ising spin glass to confirm the predicted $H_\perp$ behavior remain unclear because of the above complications.

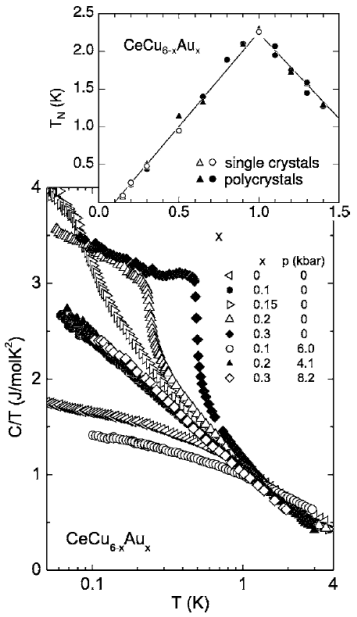

FIG. 7 Specific heat of $CeCu_{6-x}Au_x$ versus log(T) for various tuning parameters Au_x concentration and hydrostatic pressure near the QCP at x_c=0.1. Note the behavior of C/T is logarithmic at x_c signifying the QCP. There are slight deviations from FL behavior (C/T $\approx$ constant) at $x < x_c$; and weak moment, incommensurate antiferromagnetic (SDW-type) order for $x > x_c$. Pressure restores the lower x behavior, i.e., removes the AF-order and generates a return to quantum criticality and FL behavior. The upper panel traces the AF Néel temperature as a function of x for single and polycrystal samples. Note how T_N becomes reduced as x increases above 1.0. This illustrates the disorder effects of large au dilutions probably affecting the band structure and Fermi surface of $CeCu_6$. According to von Löhneysen et al. (2007).

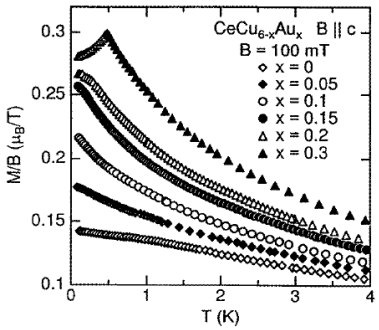

FIG. 8 Magnetic susceptibility, χ=M/H, for various concentrations of $CeCu_{6-x}Au_x$ in an easy axis magnetic field of 0.1T. Note the NFL behavior at x_c=0.1 and the antiferromagnetic peak for x=0.3. According to von Löhneysen (1996).

At present, the closest realization of transverse field Ising criticality occurs in columbite $CoNb_2O_6$, a material outside the scope of this review.(Coldea et al., 2010; Lee et al., 2010) As for rare earths and actinides, theory still greatly outweighs the "ideal" material experiments.

2. $Ce(Cu,Au)_6$

The first heavy-fermion material $CeCu_6$ was originally proposed (von Löhneysen et al., 1994) to show a QCP with combinations of different tuning parameters: Au-dilution, pressure, and magnetic field. This well-studied intermetallic compound was extensively reviewed by von Löhneysen et al. (2007). Here we briefly summarize the long history of $CeCu_{6-x}Au_x$ and relate the QPT behavior to recently evolving work. Specific heat data are shown in Figure 7, for various doping x and pressure P.

Pure $CeCu_6$ does not order magnetically down to at least 10mK. In a good Fermi liquid the specific heat C/T should

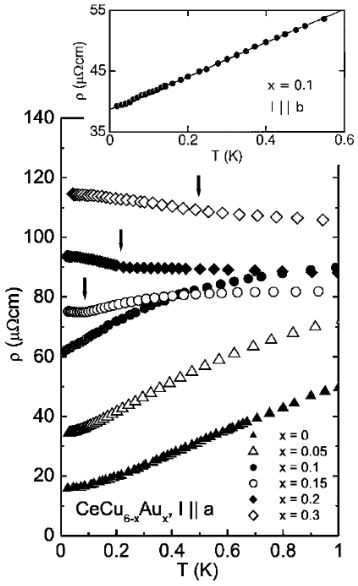

FIG. 9 Electrical resistivity, ρ, of Ce($Cu_{6-x}Au_x$) from 0 to 0.3 concentration tuning. The ρ(T) curves illustrate the change of behavior from HFL (T^2) to NFL (T) to a constant resistivity due to the strong disorder of Au_x doping. Here the antiferromagnetic transition is hardly discernible because of the large disorder scattering. According to von Löhneysen et al. (2007).

approach a constant as $T \to 0$, hence the slight upturn of C/T in Figure 7 suggests the presents of spin fluctuations disturbing the Fermi liquid.

With increasing Au-concentration the QCP is reached at $x_c = 0.1$, where the C/T behavior changes to $C/T \sim [\ln(T_o/T)]$. This temperature dependence indicates non-Fermi liquid (NFL) behavior, an indication of possible quantum criticality. By further increasing the Au concentration x magnetic order is generated. This phase is an incommensurate spin density wave(Schröder et al., 1994) with small staggered magnetic moments, reaching $\mu \approx 1.2\mu_B$/Ce at $x = 1.0$. The concentration dependence of T_N is shown in the upper panel of Figure 7. The Néel temperature T_N begins to decrease above $x = 1.0$ due to the destructive effects of disorder affecting the band structure and Fermi surface of this strongly correlated material. As a function of Au-concentration tuning we have thus have a V-shaped region of quantum criticality just above x_c, as suggested by Figure 2. Note that the putative Fermi liquid state for concentrations $x < x_c$ has not been designated.

Another thermodynamic property of $CeCu_{6-x}Au_x$is the dc bulk magnetic susceptibility χ. Figure 8 shows $\chi = M/H$ for concentrations $0 \leq x \leq 0.3$ and the magnetic field H applied along **c**. There is a near constant in T-dependence for $x = 0$ and the gradual low temperature upturn at x_c, with the antiferromagnetic order only becoming apparent at $x = 0.3$. The susceptibility behavior at the QCP follows a $\chi = \chi_0 - \delta\sqrt{T}$ dependence. Spin fluctuations seem to be modifying the $x = 0$ Fermi liquid state where χ should be constant as T $\to$ 0.

Pressure can be used to "retune" the concentration behavior, see Figure 7. This reversing behavior demonstrates that an increasing Au concentration expands the lattice, whereas pressure P compresses it. Such correspondence is limited to small concentrations and moderate hydrostatic pressures, it breaks down if x or P is too large. Nonetheless, the low temperature specific heat displayed in Figure 7 established evidence for a QCP where the critical Au concentrations x_c increases with pressure.

Next, consider the all-important resistivity as shown in Figure 9. At $x = 0$ initial Fermi liquid behavior is observed, $\rho = \rho_0 + AT^2$. The temperature dependence of the resistivity ρ becomes linear ($\rho = \rho_0 + A'T$) at the critical value $x_c = 0.1$, signaling non-Fermi liquid behavior. For $x = 0.15$ we are already in the magnetically ordered phase, with a dubious suggestion of a 'kink' in the resistivity at the spin ordering Néel temperature T_N. Disturbingly, this magnetic ordering kink is not found at higher gold concentrations, instead there is an enormous increase in the residual resistivity. This transport-property effect clearly establishes the large change in scattering rates with increasing doping, which are mainly related to the Fermi surface and band structures. Note that even at zero doping $x = 0$ there is a rather large residual resistivity!

The spin density wave (SDW), as detected by neutron scattering (Schröder et al., 1994), is a most subtle form of magnetism and the tiny x-disorder is essential to tune it. The mysterious 'Kondo hybridization' between the Ce $4f$

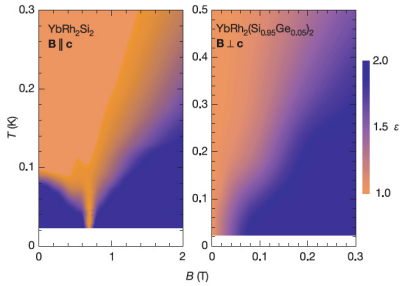

FIG. 10 Temperature versus magnetic field phase diagram of $YbRh_2Si_2$. The color contours illustrate the temperature exponent of the resistivity: red equals linear T, blue quadratic T^2 in the various field tuned regimes. According to Custers et al. (2003).

electrons and the conduction electrons compensate the moments, thereby diminish the RKKY interaction resulting in this small moment itinerant SDW.

Further inelastic neutron scattering probed the critical fluctuations at x_c (Stockert et al., 1998). The spin fluctuations appeared to be highly anisotropic leading to a rod-like formation of excitations in the dynamical structure factor $S(\mathbf{q},\omega)$. In real space this corresponds to quasi-2D fluctuations (Rosch et al., 1997). The dynamical structure factor $S(\mathbf{q}=\text{const},\omega)$ resulted in a dynamical scaling of the dynamical susceptibility in ω/T (Schröder et al., 2000). Interestingly, Hertz-Millis theory is incompatible with such ω/T scaling, indicating the need for new theories.

The third way to tune the system is through an external applied magnetic field $\mathbf{H}$. Since Au_x dilution can be reversed with hydrostatic pressure, the field tuning should have similar effects to diminish the antiferromagnetism and return the compound $CeCu_{6-x}Au_x$ to its QCP at $x_c = 0.1$. Such experiments were performed on a single crystal of $CeCu_{5.8}Au_{0.2}$ with $\mathbf{H}$ along its easy axis using specific heat and resistivity determinations. The field-tuned results could then be compared to Figures 7, 8 and 9. However, distinctly different power law exponents were observed for the field-tuned measurements (von Löhneysen et al., 2001). This behavior is consistent with the Hertz-Millis theories while, in contrast, x and P tuning required a completely different scenario.

Additional field tuning experimental were carried out on silver-doped $CeCu_{6-x}Ag_x$ (Heuser et al., 1998). However, slightly larger $Ag_x(\approx 0.2)$ concentrations are needed to start in the antiferromagnetic phase. The limited measurements are performed only on non-analyzed polycrystal samples. These authors claim that both doping and field-tuning generate the NFL behavior which is caused by an underlying QCP. One must be careful: NFL properties are not only related to quantum criticality in these strongly correlated intermetallic heavy-fermion compounds. Disorder is also a prime cause of anomalous thermodynamic and transport behavior. Additionally, the magnetic field, as a vector quantity, can induce deviations from T^2 resistivity dependences due to magnetic modes and anisotropic scattering. Similarly, discrepancies can be found in the specific heat. So we must be cautious about claiming NFL behavior is solely related to an underlying quantum critical point.

Therefore, after all is said and measured, a number of open and fundamental queries remain. Why does the field-tuning appear so much different from the pressure or doping-tuned quantum phase transition? What is the role of disorder, specifically in terms of destroying the heavy Fermi Liquid state? How does the Kondo compensation of the local moments exactly work? This last point is related to a more general question on whether the magnetic state is the result of Fermi surface or local moment effects? Then there is, finally, the question of the observed ω/T-scaling and the possible two-dimensional spin fluctuations. These ruminations represent our present-day questioning of quantum criticality in $CeCu_{6-x}Au_x$.

3. $YbRh_2Si_2$

From the opposite end of the lanthanide series, another antiferromagnetic heavy-fermion material was discovered in 2000: $YbRh_2Si_2$ (Trovarelli et al., 2000). This intermetallic compound requires ultra-low temperatures and small magnetic field ($H_c \cong 0.7$ T perpendicular to the easy axis) to reach a quantum phase transition, from a very low temperature antiferromagnetic phase ($T_N = 0.07$K and $10^{-3}\mu_B$ moment). Again, the key signatures of quantum criticality arise through non-Fermi liquid behavior, i.e., the unconventional low-T power-laws of the resistivity, specific heat and susceptibility. For $YbRh_2Si_2$ the NFL (quantum critical) regime spans the entire temperature-field phase space, above the QCP and even above the antiferromagnetic phase.

Figure 10 exhibits this phase diagram based on resistivity measurements(Custers et al., 2003). On the left side the field is applied along the hard direction $H \parallel c$, which requires a field of 0.7 T to reach the QCP. As indicated by the resistivity's T-exponent ϵ, there is a large region of NFL behavior throughout most of the phase diagram. The color

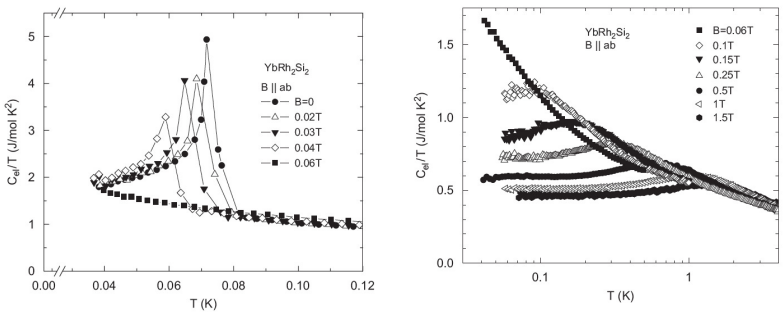

FIG. 11 Specific heat in various magnetic fields for $YbRh_2Si_2$, left: low fields $H \leq 0.06$T; right: $H \geq 0.06$ T $= H_c$. Note the quenching of antiferromagnetic order ("lambda transition") with field and the logarithmic upturn that becomes constant at very large fields. According to Oeschler et al. (2008).

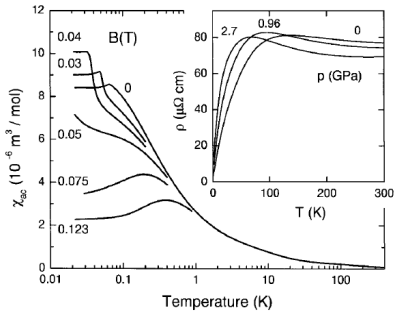

FIG. 12 ac-susceptibility of $YbRh_2Si_2$ in small magnetic field approaching the QCP. χ_{ac} gives indications of ferromagnetic freezing in small fields that become smeared out as the eternal field is increased. The inset shows the full ρ(T) behavior with the large high T resistivities and minimum pressure dependences. According to Trovarelli et al. (2000).

coding illustrates how the T^{ϵ} changes from 2 (Fermi-liquid) to 1 (non-Fermi liquid). On the right Ge alloying is used to expand the lattice, thus reducing T_N, such that the critical field along the easy axis is reduced to $H_c \cong 0.027$ T. For small concentrations of Ge, here 5%, the lattice disorder and strain is expected to be minimal.

The specific heat, plotted as C/T versus T and logT, is illustrated in Figure 11 for different applied fields along the easy axis (Oeschler et al., 2008). The enhanced antiferromagnetic peak at T_N is reduced in both temperature and magnitude with applied field H, until it disappears at the QCP, now at $H_c \cong 0.06$ T.

The expected non-Fermi liquid behavior $C/T \sim \log(T_0/T)$, becomes steeper for low temperatures $T < 0.3K$ where it turns into a power-law $C/T \sim T^{-0.3}$. This suggests another entropy contribution, probably from hyperfine interactions resulting from the nuclear magnetism of the Yb nucleus. At larger H-fields C/T is essentially constant, indicating Fermi liquid behavior.

The ac susceptibility and magnetization of $YbRh_2Si_2$ show deviations from their high-temperature Curie-Weiss (C-W) behavior. Figure 12 shows the ac-susceptibility for $YdRh_2Si_2$ at various magnetic fields (Trovarelli et al., 2000).

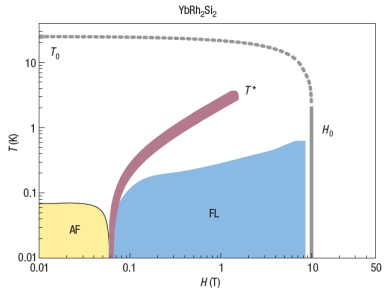

FIG. 13 Extended logT(K) vs logH(T) phase diagram of $YbRh_2Si_2$ as function of magnetic field (in-plane, easy) illustrating the QCP, AF, NFL and Lifshitz transition phases. Note the $T*$ line that is used to denote the Kondo breakdown scale, extracted from Hall measurements, and the T_C line illustrating the formation of the HFL. According to Gegenwart et al. (2008).

The small peak in zero field followed by flatness denote the tiny moment antiferromagnetic transition. Above the Néel temperature T_N one can already observe the precursor discrepancy in an upturn away from the C-W form. With increasing field the weak power-law behavior becomes noticeable, e.g. at 0.05 T. However, at the lowest temperature there is a stronger increase in χ_{ac} due to the nuclear contribution. The dc-magnetization divided by field, M/H, shows a similar upturn at the critical field H_c that becomes less strong, finally reaching a flat $M/H(T)$ at 0.3 T (Tokiwa et al., 2009). Because a C-W analysis is invalid for this strongly correlated and fluctuating low-temperature regime, highly sophisticated analysis must be used to treat the data and extract physical conclusions (Abrahams and Wölfle, 2012).

Since the Néel temperature and critical fields are so small it is most difficult to perform microscopic measurements below T_N and around H_c. Therefore most experimental probes at temperatures below 0.07K are limited to transport or thermodynamic measurements. The Hall effect tuned with the two field directions has been examined in detail by Paschen et al. (2004), which results in the overall phase diagram in Figure 13(Gegenwart et al., 2008). The Hall coefficent R_H shows an change at a 'crossover' line $T*(H)$ line that seems to extrapolate to a sudden jump in R_H at zero temperature. Further experiments tracked the thermopower $S(T,B)$ in the field and temperature region surrounding the QCP (Hartmann et al., 2010). Here an agreeing crossover feature, namely a change of sign, at the $T*(B)$ line was observed in $S(B)/T$. However, the general behavior of $S(T,B)/T$ is rather complicated with significant scatter thereby preventing a full understanding.

Experiments of the Grüneisen ratio $\Gamma = (V_{mol}/\kappa_T)(\alpha_{cr}/C_{cr})$ and magnetic Grüneisen ratio $\Gamma_{mag} = -(dM/dT)/C$, i.e., the magnetocaloric effect $(1/T)(dT/dH)$ at constant entropy, were performed by Küchler et al. (2003) and Tokiwa et al. (2009), respectively. Inverse power-law divergences were generally found indicating a quantum phase transition as predicted by theory (Zhu et al., 2003), see Sec. II.C.

Finally, inelastic neutron scattering (INS) experiments were carried out in magnetic fields down to temperatures of $T \sim 0.1$ K, which is still above T_N, by (Stock et al., 2012) to probe the NFL state of $YbSi_2Si_2$. These dynamical resonances detect the spin fluctuations in the meV energy range and their momentum dependence within the Brillouin zone. The zero-field spin fluctuations are incommensurate in the basal plane with ferromagnetic interplane correlations. There is a strong dependence of the fluctuation spectra with temperature due to the competition between ferromagnetic and incommensurate antiferromagnetic components. In large magnetic fields, e.g., $H \sim 2-10$ T, local moment behavior is field-induced that can be interpreted as localized droplets of Yb^{+3} spins extending on a length scale of $\sim 10\mathring{A}$. This response indicates a change in behavior for low-field itinerancy, i.e., Fermi surface nesting, to Kondo screened local moments (Stock et al., 2012).

A very recent NMR study of the spin-lattice relaxation time, T_1, of ^{29}Si spanning the QCP (Kambe et al., 2014) has concluded that a coexistence of both heavy Fermi liquid (HFL) and non-Fermi liquid (NFL) phases exist. These paired states represent an itinerant HFL component degenerate at the QCP with a localized NFL whose ratio $R(T,H) = f_{\rm NFL}/f_{\rm HFL}$ varies with T and H. The description assumes a 'two-fluid' scaling relation that nicely fits the data with reasonable scaling exponents. Thus we have a novel interpretation that adds a new element to the quantum critical behavior, yet it leaves the antiferromagnetic state, the putative spin-density wave, unresolved with both quantum critical ferromagnetic and antiferromagnetic fluctuations playing a role (Kambe et al., 2014).

So what then is nature of the antiferromagnetic transition below 0.07K and how is this state perturbed with tiny fields of ∼0.06T to create the quantum critical point? Additional microscopic or local experiments, such as ARPES, STM/STS, quantum oscillations, core spectroscopy, etc., are needed to answer this question. Although an enormous amount of effort and manpower resulting in many premier publications have been devoted to $YbRh_2Si_2$ and its QCP, the exact causes and their description have remained incomplete.

Note that there are other ytterbium-based heavy fermion materials that exhibit quantum criticality. A recent example is $YbNi_4(P_{1-x}As_x)_2$, which is an itinerant ferromagnet that can be tuned to criticality by either a magnetic field or arsenic doping. A divergence of the Grüneisen ratio was found, inconsistent with the Hertz-Millis predictions.(Steppke et al., 2013)

III. PRESENT THEORIES

A. Critique of Hertz-Millis and the Kondo effect

As discussed in the previous section, both $CeCu_{6-x}Au_x$ and $YbRh_2Si_2$ display features that are incompatible with standard Hertz-Millis theory. This forces us to look at reasons why this itinerant spin-density wave picture should not apply.

The most fundamental critique originates in the microscopic nature of the materials. In addition to the usual set of conduction electrons, the materials of this Chapter contain electrons localized in f-orbitals. The interaction between conduction electrons and localized d or f-states was first studied by Kondo(Kondo, 1964), who introduced the model

of a single magnetic impurity in a metal,

$$H = \sum_{k\sigma} \epsilon_k c^\dagger_{k\sigma} c_{k\sigma} + J\vec{S}\cdot\vec{s} \tag{19}$$

where $\vec{S}$ is the spin of a localized impurity, k is the electron momentum with dispersion ϵ_k, and $\vec{s} = \sum_{kk'} c^\dagger_{k\alpha}\vec{\sigma}_{\alpha\beta}c_{k'\beta}$ is the total spin of the conduction electrons at the impurity site. At temperatures below the Kondo temperature $T_K \sim \exp(-1/JN_0)$, where N_0 is the density of states of the conduction electrons at the Fermi level, Kondo showed that the localized spin forms a singlet state with the conduction electrons. This process of Kondo screening effectively delocalizes the initially localized f-electron.(Anderson, 1970; Hewson, 1993; Kondo, 1964)

It was expected that Kondo hybridization will also occur in materials that have localized f-electrons in every unit cell. The corresponding Kondo lattice model (Doniach, 1977)

$$H = \sum_{k\sigma} \epsilon_k c^\dagger_{k\sigma} c_{k\sigma} + J\sum_i \vec{S}_i\cdot\vec{s}_i \tag{20}$$

is suggested to be a standard Fermi liquid below the Kondo coherence temperature T_{coh}. Below this temperature, the f-electrons are hybridized with the conduction electrons, and the effective mass of the new electrons is drastically enhanced: a 'heavy' Fermi liquid (HFL). The delocalization of the f-electrons implies that the Fermi surface becomes larger than it would be when only the c-electrons would be mobile.(Oshikawa, 2000)

Even though the Kondo lattice model has been studied extensively with various methods (such as slave-boson theory(Burdin et al., 2000), for further reading see Sec. II.F.2. of von Löhneysen et al. (2007)), there is currently no solid understanding of how the hybridization of f- and c-electrons works. This lack of understanding then carries over to the realm of Hertz-Millis (HM) theory that requires simple Landau fermi-liquid quasiparticles to start with.

Nevertheless, the notion of a quantum critical point in a Kondo lattice system can be introduced. Antiferromagnetism in the Kondo lattice model can arise from interactions between the f-electrons, mediated by the c-electrons.(Kasuya, 1956; Ruderman and Kittel, 1954; Yosida, 1957) This Ruderman-Kittel-Kasuya-Yosida (RKKY) interaction at energy scale $E_{RKKY} \sim J^2N_0$ competes with the Kondo screening at $T_K \sim \exp(-1/JN_0)$, leading to a quantum phase transition as a function of the coupling J.

B. Kondo breakdown

A more radical idea involves a breakdown of the Kondo hybridization at the critical point. There are some strong experimental evidences that hint in such a direction, for example the divergence of the effective mass as exemplified by the diverging specific heat coefficient C/T and the existence of T^*-line in $YbRh_2Si_2$. Although the idea is certainly appealing, again it seems very difficult to extract quantitative predictions based on the scenario of the Kondo breakdown.(Coleman, 1999, 2001; Coleman et al., 2001; Coleman, 2015; Sengupta, 2000; Si et al., 2001, 2014)

The theories of Kondo breakdown originate from dynamical mean field theory (DMFT) (Georges et al., 1996), a numerical technique where the order parameter is still local in space but can have nonlocal temporal correlations. In addition to the critical fluctuations associated with the antiferromagnetic order, in the Kondo breakdown there are also purely local critical fluctuations associated with the localization of the f-electrons.

The most important prediction of the Kondo breakdown scenario is the existence of a large Fermi surface on right side of the transition, encompassing both f- and c-electrons, whereas on the antiferromagnetic (left) side of the transition the Fermi surface is 'small' and only contains c-electrons. So far there is no direct experimental evidence, for example ARPES(Kummer et al., 2015; Paschen et al., 2015), that supports this claim. Indirect evidence, such as the T^* line based on a crossover in the Hall conductivity, can also be explained differently.

Some authors have gone even further by completely discarding the antiferromagnetic transition and focussing on an isolated Kondo breakdown. In this picture the localized f-electrons will form a spin liquid, coexisting with a small Fermi surface metal dubbed FL^*.(Senthil et al., 2003, 2004) Antiferromagnetic order would then be an instability of this FL^* phase. The absence of two different transitions suggests this exotic theory is not relevant for experiments.

C. Two dimensional physics

A surprising caveat of the Kondo breakdown pictures is that requires the system to be effectively two-dimensional.(Si et al., 2001) In fact, many features of $CeCu_{6-x}Au_x$ such as the logarithmic divergence of the specific heat coefficient

can be understood by $d = 2$-dimensional Hertz-Millis theory.(Rosch et al., 1997) It is quite puzzling, however, since there is no apparent microscopic reason why these materials would be highly anisotropic.

In additiion, later it was found that standard Hertz-Millis theory develops some anomalies in two dimensions that render it incorrect. This originates from the fact that antiferromagnetic fluctuations ($z = 2$) in two dimensions have effective dimension $d + z = 4$, exactly the upper critical dimension where interactions become marginally relevant. It has been found that one cannot integrate out fermions to arrive at an effective model, as Hertz originally did. Instead, both electrons and critical fluctuations need to be treated at an equal level, which is an ongoing theoretical effort.(Abanov and Chubukov, 2000, 2004; Lee, 2009; Metlitski and Sachdev, 2010; Pankov et al., 2004; Varma, 2015).

D. Critical quasiparticles

While Kondo hybridization certainly takes on an important role in many heavy fermion compounds, an alternative approach to the Kondo breakdown picture is to describe the effective mass divergence phenomenologically. The quasiparticle mass enhancement is characterized by the parameter $Z = m/m^*$, and hence experimentally we find $Z \to 0$ at the transition. This would naively imply that the Fermi surface and hence the materials metallic behavior would disappear. Yet, the way around this is via a 'critical' Fermi surface(Senthil, 2008) where $Z = 0$ but the spectral function still displays some kind of nonanalytic behavior. One can write down phenomenologically the Greens function for the corresponding critical quasiparticles(Abrahams et al., 2014; Vojta et al., 2015; Wölfle and Abrahams, 2011, 2015), from which many critical exponents can be extracted that match experimental results. Nonetheless, a microscopic picture of why quasiparticles would become critical is still lacking.

E. Conclusion

The theoretical field seems to be in a state of confusion. At the one hand there are microscopic models based on Kondo physics between f- and c-electrons, but those seem to be nearly impossible to solve rigorously. On the other hand it is possible to describe a number of experiments by purely phenomenological models. It remains a challenge for the theorists to find a good microscopic basis for their phenomenology. In addition, new experimental results such as ARPES at low temperatures, are then necessary to distinguish between different scenarios of quantum criticality beyond Hertz-Millis.

IV. PRESENT MATERIALS AND EXPERIMENTS

There are numerous lanthanide-based heavy-fermion liquids that are claimed to exhibit QPT's. Rather than attempting to catalogue and evaluate these many different materials and their quantum criticality claims, we offer here some overview articles where the reader can find these intermetallic compounds and extract the experimental details. For up-to-date reference we refer to the following reviews by Stewart (2001, 2006), Coleman and Schofield (2005), von Löhneysen et al. (2007),) Gegenwart et al. (2008), Pfleiderer (2009), Si and Steglich (2010), and Stockert et al. (2011).

In order to create and study a QPT, the general protocol consists of reducing with pressure, magnetic field, frustration and/or dilution the magnetic or superconducting phase to $T = 0$. Here the *a priori* question arises, whether such tuning leads to a continuous quantum phase transition? The usual justification for a QCP is the appearance of NFL behavior instead of standard Fermi liquid behavior. However, other types of transitions without these quantum fluctuations could occur, e.g., droplets, inhomogeneties, percolation or glassy dynamics (Seo et al., 2014). So additional criteria beyond the NFL effects are needed to characterized the near T→0 behavior, e.g., the use of the Grüneisen ratio, see Sec. II.C.

In both the Cerium-based series Ce(Co, Rh; Ir)In_5 and the uranium compound URu_2Si_2, distinct non-Fermi liquid behavior has been observed. We will now address the question whether this NFL behavior can be ascribed to a quantum critical point.

A. The Cerium series Ce(Co, Rh; Ir)In_5

Let us now focus on an intensely studied Ce-system, viz. Ce(Co, Rh; Ir)In_5 where a variety of behavior and tunings have been investigated. $CeCoIn_5$ is a heavy-fermion superconductor with $T_c^S = 2.3$ K that is claimed to be magnetically mediated (Petrovic et al., 2001b). Pressure was then applied to destroy the superconductivity at ≈ 3.5 GPa preceded by an anomalous change in the transport properties at 1.6 GPa where T_c^S reaches a maximum of 2.6

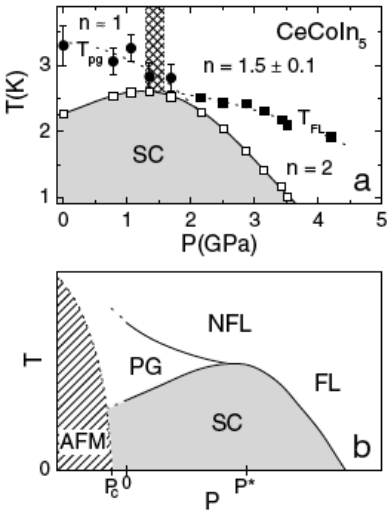

FIG. 14 Upper panel: Temperature - pressure phase diagram of $CeCoIn_5$ determined by electrical resistivity. A QCP is expected at $P_{QPT} = 3.5$ GPa but it emerges from a FL state instead of a NFL. Lower panel: Proposed schematic of various T - P phases. Note that the AFM only appears at negative pressures and the speculations of a pseudogap. According to Sidorov et al. (2002).

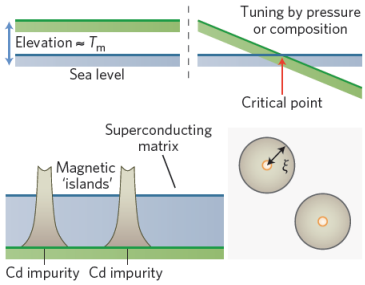

FIG. 15 Cartoon of the Cd doping effect on $CeCo_5$, model of Seo et al. (2014). Upper left: The AFM state (green) lies favorable above the SC (sea-level) state. Upper right: By tuning the pressure or composition a QCP can be created by reducing thew AFM state below the SC state. Lower left: Cd doping produces magnetic islands with in the SC matrix. Lower right: If the magnetic correlation length exceeds the distance between islands, long-range AFM occurs via percolation. Cartoon according to Grosche (2014).

K (Sidorov et al., 2002). However, an anticipated antiferromagnetic phase was only speculated to exist at 'negative' pressures. Figure 14 shows the proposed temperature - pressure phase diagram for $CeCoIn_5$ (Sidorov et al., 2002).

Since pressure tuning did not find the antiferromagnetic order, this then encourages magnetic-field tuning to drive $T_c^S \rightarrow 0$, as detected by magnetoresistance measurements. Here phase diagrams were proposed with a QCP at the destruction of superconductivity (SC), yet before the onset of Fermi liquid behavior (Paglione et al., 2003). A similar phase diagram was established by Bianchi et al. (2003) from field dependent specific heat and resistivity data, including crossovers from superconducting to NFL to FL behavior. The interpretation of the QCP at 5 T was related to field-tuned antiferromagnetic spin fluctuations. However, the attempt to directly detect signs of antiferromagnetism failed.

The remaining tuning parameter for $CeCoIn_5$ is doping, and specifically to substitute Cd on the In sites to effectively remove electrons. In the $In_{(1-x}Cd_x)_5$ experiments, the parameter x refers to the nominal rather than the actual Cd concentration. Indeed AFM order develops with Cd_x for x > 7.5% as detected via specific heat and resistivity (Pham et al., 2006). In addition of superconductivity being depressed with Cd doping, there seems to exist overlaps with the antiferromagnetic order, suggesting possible inhomogeneous phases. In order to probe the AFM and SC on a local scale, NMR was employed to study the extent of these phases (Urbano et al., 2007). Here the results are interpreted in terms of local droplets of magnetism surrounding the Cd impurities. With a sufficient concentration of droplets, that is, cadmium, a percolative transition occurs towards true long-range AFM within the coexistent superconductivity matrix. Further details concerning the dangers of disorder caused by impurity doping is discussed

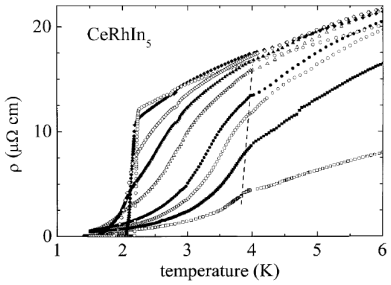

FIG. 16 Pressure induced superconductivity and destruction of antiferromagnetism in $CeRhIn_5$ determined via resistivity with pressure increasing vertically from 0 to 21 kbars. From $d\rho/dT$ the antiferromagnetic transition temperature T_N can be found, and the superconducting transition T_c occurs when $\rho = 0$. According to Hegger et al. (2000).

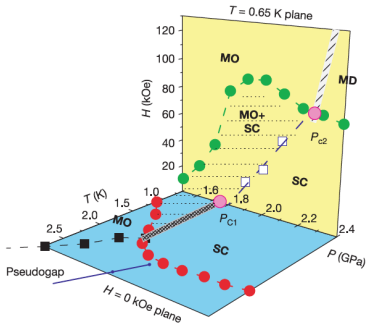

FIG. 17 Magnetic field, temperature, and pressure phase diagram of $CeRhIn_5$. The $T = 0.65$ K plane represents the extrapolated $T = 0$ QCP. Here lines of phase transitions are expected between magnetically ordered (MO) to coexisting magnetic order with superconductivity (MO+SC) to a superconducting phase (SC), and finally a high field magnetic disordered state (MD). Note the tetracritical point at Pc2. According to Park et al. (2006).

by Seo et al. (2014). Currently their droplet model is probed by nuclear quadrupole resonance (NQR) on a local scale. A cartoon illustration of the pressure dependence of the AFM droplets is shown in Figure 15. This nucleation interpretation emphasizes the the annulling effect of disordered ligand doping on the quantum criticality. For instead of a homogeneous QPT we now create a freezing of magnetic fluctuations generating an inhomogeneous glassy ground state. In summary: the doped system seems to display not a proper QPT but rather a frozen quantum glass.

Another compound, $CeRhIn_5$, is antiferromagnetic with $T_N \approx 3.8$ K as determined by C/T, χ, and ρ measurements. Neutron scattering has detected an incommensurate spiral magnetic structure with $0.26\mu_B$ Ce-moments (Bao et al., 2000). Under pressure T_N slowly decreases, however, above 1.5 GPa $CeRhIn_5$ becomes superconducting with $T_c^S = 1.9$ K. There exists seemingly a bulk heavy-fermion antiferromagnet to superconductivity crossover (Hegger et al., 2000). Figure 16 exhibits the resistivity as a function of temperature at different pressures, the $d\rho/dT$ maxima denote the magnetic transition temperature T_N and $\rho = 0$ at $T = 2$ K signals the SC state. Unfortunately, unknown anomalies also exist within the temperature - pressure phase diagram, yet the AFM vanishes at a certain pressure $P_{c1} = 1.77$ GPa when the Néel temperature equals the superconducting critical temperature, $T_N = T_c^S$. Below P_{c1} there seems a small region of coexistence.

Magnetic field tuning can be combined with pressure tuning, for such systems the specific heat C/T was measured as a function of T, P and H (Park et al., 2006). The resulting 3D phase diagram is shown in Figure 17. If we take the $T = 0.65$ K plane to approximate $T = 0$, the data points lying in this plane represent the proposed QCP's. With increasing H and P a line of QCP's separates the antiferromagnetic phase (MO) from a region of coexisting MO and SC. At $H = 0$ a QCP is formed at P_{c1}.

Additional $C/T(T, P)$ measurements were carried out by Knebel et al. (2006) that showed an inhomogeneous SC/AFM state followed, at a higher pressure, by pure SC. With increased H and P a second 'tetracritical' quantum point is reached at $P_{c2} = 2.25$ GPa. However, there are little or no experimental data for the temperature dependences, that is, whether there is NFL behavior or if the various coexistence phases are homogeneous or disordered. Nevertheless, Park et al. (2006) attempt to draw similarities with the high-T_c cuprates even though the putative QPT's are undefined. An interesting experiment here is the de Haas-van Alphen studies of the Fermi surface as a function of pressure (Shishido et al., 2005). The authors observed an increase in the cyclotron mass above 1.6 GPa,

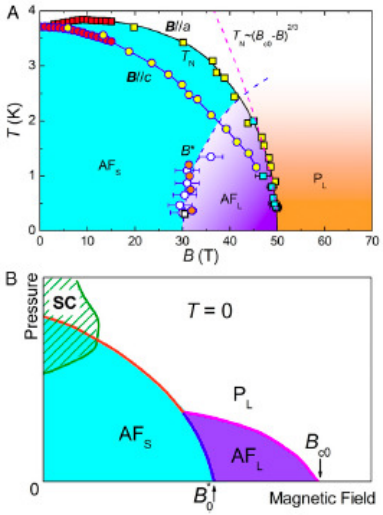

FIG. 18 High field phase diagrams for $CeRhIn_5$. Upper panel: Temperature versus field phase diagram down to 0.5 K and up to 50 T, illustrating the change from a small Fermi surface in AF_S to large Fermi surface in AF_L. P_L represents a large Fermi surface paramagnet. Lower panel: Proposed pressure versus field phase diagram at $T = 0$. Note the coexistence of of superconductivity (SC) and antiferromagnetism (AF). According to Jiao et al. (2015).

where superconductivity sets in. Above 2.4 GPa a drastic reconstruction of the Fermi surface occurs that indicates a change from localized to itinerant behavior thereby giving a T_c^S maximum.

Finally and most recently very high magnetic fields (H to 70T) have been applied to investigate the quantum oscillations, specific heat, and Hall effect of $CeRhIn_5$ (Jiao et al., 2015). These authors observe field-induced modifications of the phase coincident with sharp reconstructions of the Fermi surface (FS) in all the high-field measurements. Especially dramatic are the changes in the quantum oscillation as a function of field H, spanning 10 to 30 T and 45 to 70 T. Based on the data an experimental phase diagram ($T - H$) may be constructed as shown in Figure 18 – contrast with Figure 17. Although the lowest temperature of measurement is only $\approx$ 0.4K, when extrapolated to $T = 0$, two quantum critical points are proposed: the transition from an AFM with a small Fermi surface (AFM_S) to one with a large Fermi surface (AFM_L) at $\approx$ 30 T; and a transition from an antiferromagnet to a paramagnet (P_L) at $\approx$ 50T. The authors speculate further with a 'schematic' pressure - field phase diagram at $T = 0$ for $CeRhIn_5$. Here there are intersecting quantum critical lines in between SC, AFM_S, AFM_L, and P_L phases as illustrated in the bottom half of Figure 18. These conjectures of quantum critical lines warrant their experimental proof.

The last in this cerium-troika, $CeIrIn_5$, is a heavy-fermion unconventional superconductor with $T_c^S = 0.4$ K lacking any coexisting magnetic order (Petrovic et al., 2001a). Accordingly, the superconductivity was thought to be mediated by valence fluctuations rather than by spin fluctuations. Thermal conductivity and penetration depth studies indicate a $d_{x^2-y^2}$ - type gap symmetry (Movshovich et al., 2001) and (Vandervelde et al., 2009). Recent doping investigations of Hg and Sn on In sites, and Pt on Ir sites were performed using C(T) and ρ(T) (Shang et al., 2014). The results indicated hole doping via Hg caused AFM while electron doping via Sn or Pt favored a paramagnetic Fermi-liquid. Again the microprobe-determined concentrations are significantly different from the nominal concentrations. So disorder and clustering could be the main cause of the AFM and FL behavior. All of which appears out of a NFL regime.There was no evidence of QPT or QCP for $CeIrIn_5$ or its various doping.

B. Hidden order in URu_2Si_2

There is a particular uranium-based heavy fermion intermetallic compound, URu_2Si_2, that has been studied in-detail regarding a possible quantum phase transition. URu_2Si_2 is well-known as the hidden order (HO) material which shows a mysterious continuous phase transition at 17.5 K. The origin of this transition is neither magnetic nor structural and still persists after 30 years as unclarified, thus its designation as hidden order. Only within the HO phase does unconventional superconductivity exists below $T_c = 1.5$ K. Much has been published, both experimentally and theoretically, in relation to the HO state and its formation (Mydosh and Oppeneer, 2011, 2014).

From an experimental point of view, the hidden order has stimulated the developments of novel methods to detect its origin. In Figure 19 we show an 'elephant' cartoon of these many techniques utilized to characterize the HO. There has been significant progress in developing exotic evaluations of the HO beyond the bulk studies. For the

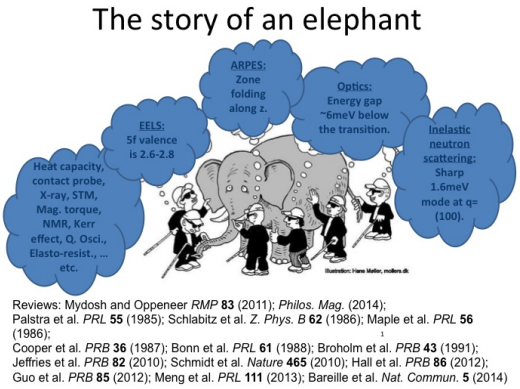

FIG. 19 Overview cartoon illustrating the many experiments and references on the blind man's elephant searching for the meaning of hidden order in URu_2Si_2 . According to Kung, unpublished.

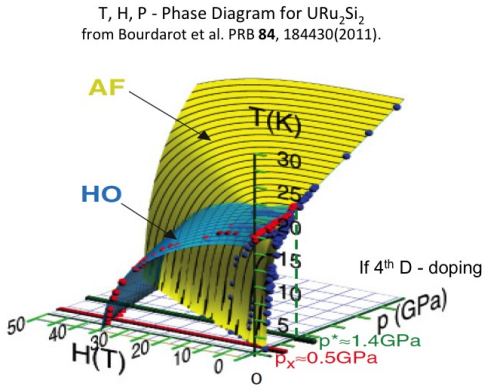

FIG. 20 3D phase diagram od URu_2Si_2 illustrating the different phases (HO. AFM, SC, and HLF) and the possibilities for tuning towards a QCP. Note that the 4th dimension of doping has been omitted. According to Bourdarot et al. (2011).

first time ARPES, STM/STS, magnetic torque, Raman, polar Kerr, cyclotron resonance, elasto-resistivity and core-level spectroscopy have been applied to a heavy fermion system. Furthermore, theorists have proposed more than 30 different models and interpretations to describe the hidden order. High-ranking multipole orders are a favorite interpretation (Kung et al., 2015; Mydosh and Oppeneer, 2014).

Pressure, magnetic field and doping have been employed to tune the HO and SC towards quantum criticality. In Figure 20 we show the 3D phase diagram as a function of T, H and P, omitting the many different dopings or substitutions that require a 4th dimension. The disordering of the delicate HO state via doping causes a slow

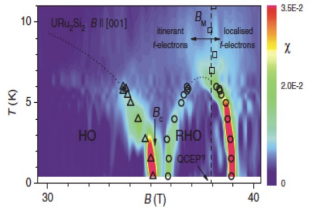

FIG. 21 High magnetic field phase diagram for URu_2Si_2 showing the destruction of HO and the creation of a then unknown Phase III. Above the dome of III the is a metamagnetic effect in the susceptibility that disappears once the dome is formed. Note the first order transition at the base of the HO and the dome. We now know phase III domb represents a long-range-order ferrimagnetic structure. According to Harrison et al. (2003).

crossover to magnetism and heavy Fermi liquid behavior. Hence the 'puddling' of these inhomogeneous states precludes the formation of continuous and well-defined QCP. Pressure creates a first-order transition towards a long-range antiferromagnetic phase which has been studied with quantum oscillations and neutron scattering (Hassinger et al., 2010; Villaume et al., 2008). Here the Fermi surface remains constant with the transition from HO to AFM. Perhaps with negative pressure we could search for QPT's (Pfleiderer et al., 2006). Therefore, the remaining tuning parameter is magnetic field H along c-axis. Figure 21 illustrates the high-field tuning of URu_2Si_2 requiring 40 T to complete, a great experimental challenge (Harrison et al., 2003). During the past 25 a variety of exotic high field techniques have been developed to study the novel phases originating between 33 and 38 T. Is the destruction of hidden order at 32T a QCP? The answer is no, because of its first-order nature. Then there is a dome called 'Phase III' whose top is second order, but end points first order. An early proposal was an hidden QCP, a metamagnetic end point, extrapolated under the dome to $T = 0$ – see Figure 21. Most recently Bragg neutron scattering has been performed in fields up to 40T, and thus a local magnetic order clarification of Phase III became available. The result is that Phase III is a long-range AFM state, thereby removing the necessity for a quantum critical endpoint (Knafo, 2015). A way of reducing the fields needed for Phase III is to dope Ru sites with a small amount (4%) of Rh (Kuwahara et al., 2013). This leads to a complete destruction of the hidden order, yet Phase III remains intact. Magnetic Bragg-peaks confirmed the AFM as now found for pure URu_2Si_2 (Kuwahara et al., 2013).

Therefore, with Phase III fully established as long-range AFM, there seems to be no quantum phase transition in URu_2Si_2.

V. QUANTUM CRITICALITY BEYOND RARE-EARTHS AND ACTINIDES

The concept of quantum criticality extends beyond the rare earth and actinide materials discussed in the previous sections. We wish to provide, for the interested reader, a brief list of other putative QCP's. Much of the proposed quantum critical behavior is spin-based, and occurs in magnetic transition metal compounds.

- There has long been the claim of a QCP in the high temperature cuprate superconductors, beneath the superconducting dome. From the theoretical prospective, see Sachdev (2003) and the experimental works of Valla et al. (1999) and Broun (2008). A very recent review of putative QCP's in the copper-oxides is by Keimer et al. (2015). Also the more recently discovered pnictides (Fe-based compounds) have been reviewed by Shibauchi et al. (2014) with again evidence for a QCP lying beneath the superconducting dome.

- Bose-Einstein condensation of magnons in quantum magnets offers another route towards QCP via magnetic field tuning. It has been suggested in mainly oxide compounds with $3d$ transition metals, and has been studied intensively during the last twenty or so years with a complete review by Zapf et al. (2014). Here there is clear evidence, both theoretically and experimentally, of quantum phase transitions with surprising behavior at the QCP.

- Low dimensional spin insulators, i.e., Ising and Heisenberg chains and ladders, are tunable with a magnetic field towards a QPT. In this regime there is a wide variety of quantum behavior, from Luttinger liquids to dimensional crossovers. Accordingly, there are the 1D topics of perturbations of the lattice, various magnetic couplings, Ising or Heisenberg class, spin gaps for integer ($S = 1$) and half-integer ($S = 1/2$) spins, and different prototypes of QCP's. Complete reviews of 1D quantum magnetism are by Giamarchi (2004) and Mikeska and Kolezhuk (2004). A more recent brief overview of quasi-one-dimensional systems is by Giamarchi (2010).

- Quantum spin liquids are usually created with frustration and can occur without a quantum phase transition but they can also be tuned towards a QCP. The spin liquids represent a most unconventional state of matter that are being sought in real systems. For a highly frustrated metallic spin liquid, e.g., $Pr_2Ir_2O_7$, a QCP has been proposed from quantum critical scaling of the Grüneisen ratio (Tokiwa et al., 2014). Strong spin-orbit interactions in competition with the magnetic exchange energy form a new tuning parameter. A recent review of the spin liquids is by Balents (2010).

- Metallic $Sr_3Ru_2O_7$ possesses a field-tuned dome-like phase around $H \approx 8$ T. By scanning the field a QCP can be created in two distinct ways: via a metamagnetic transition into the dome extrapolated to $T = 0$; or at the edges of the dome along the $T = 0$ abscissa where there are two putative QCP's denoting the left and right sides of the dome. Very recently a field-tunable antiferromagnetic SDW has been observed in the dome phase (Lester et al., 2015). This would exclude the extrapolated "metamagnetic" QCP and emphasize the the dome end points as QCP's.

- Itinerant nearly ferromagnets compounds, e.g., $ZrZn_2$ and MnSi can be driven with pressure to a disordered state. However, the putative QCP is of first order. Thus, such transitions do not represent the continuous QPT

we studied in this Chapter. Only a year ago a new itinerant compound YFe_2Al_{10} (Wu et al., 2014) was proposed to show a continuous QPT without any tuning. This material does not magnetically order down to 0.1K and an array of bulk measurement and scaling relations at low temperatures offer evidence that YFe_2Al_{10} is special example of a 2D compound where, due to quantum critical fluctuations, its ferromagnetic order is reduced to nearly 0K. Additional experiments at yet lower temperatures and tuning, for example, (negative) pressure and doping are required to generate the putative ferromagnetic transition at finite temperatures.

We have thus far listed only magnetic or spin-based quantum phase transitions. There are also numerous non-magnetic quantum phase transitions, which include the following.

- Quantum ferroelectrics, such as $SrTiO_3$ and $KTaO_3$, exhibit a lattice transition with a ferro-aligned spontaneous electric polarization, $\mathbf{P}$. The quantum tuning parameter is the ratio of the a/c lattice constants divided by the Debye wavevector, Λ^2. A recent review of this ferroelectric behavior and more analysis is given by Rowley et al. (2014).

- Conductor-insulator quantum phase transitions have been treated for a variety of materials including metal-insulator transitions (MIT) in different dimensions, Anderson localization, superconducting-insulator transitions, etc. by Dobrosavljevic et al. (2012). This is a rather old field of study that has recently been considered from the modern QPT/QCP viewpoint.

- Quantum dots are nanocrystals made of semiconductor materials that are small enough to exhibit quantum mechanical behavior. When formed in various sizes they emit different colors of light. Now the practical applications are apparent, e.g., solar cells, lighting and TV (LCD) display technologies. Due to nanostructuring lithography tiny area devices may be formed of a two-dimensional electron gas (2DEG) tuned with superimposed gates and nearby contacts that mimic the bulk Kondo effect. Here it is required to place an odd number of electrons bearing spin on the dot. For sufficiently small dots a single electron (spin=1/2) will generate the Kondo resonance behavior (Rau et al., 2010) and more recent (Amasha et al., 2013).

- In ultra-cold gases all thermal fluctuations are frozen out, only remaining are the quantum fluctuations and thus the possibility of QPT/QCP. For example, a QPT has been observed from a superfluid to a Mott insulator (Greiner et al., 2002). While limited in experimental observational techniques, the detectable spatial resolution from a 'spread out' coherent gas to localized gas of atoms at each lattice site characterizes the transition. The tuning parameter is the depth of the lattice potential. A review of such many-body cold-gas physics is given by Bloch et al. (2008).

- Two-dimensional superconducting Josephson-junction arrays form a model system with which to study quantum dynamics and QPT. Basically there are two competing energy scales: the Josephson energy associated with the coupling of Cooper pairs between the superconducting islands; and the charging energy necessary to add an an extra electron to a neutral island. By tuning these combinations one can generate a superconductor to insulator QPT, along with associated vortex dynamics (Fazio and Van Der Zant, 2001). A magnetic field or disorder can also be used to tune the Josephson array to a QCP. Presently graphene is being overlaid over superconducting discs and gate tuned to reach the QCP (Han et al., 2014).

VI. SUMMARY AND CONCLUSIONS

In this Chapter we have introduced quantum criticality and its manifestations of phase transitions in rare-earth compounds. These $T = 0$ K phase transitions are created by quantum fluctuations that can be tuned by pressure, doping or disorder, frustration, and magnetic field. The effects of the change of phase reveal themselves at finite temperatures in the basic experimental properties of specific heat, resistivity and magnetic susceptibility. We have summarized the theoretical background and synopsized the latest controversial developments. Rather than focusing on the many materials that are claimed to exhibit quantum phase transitions at a quantum critical point, we discuss a few well-studied examples with critique of the experimental shortcomings. Some illustrations of quantum criticality beyond the rare-earths are offered in the final section.

Generically speaking there are certain limitations with all the possible tuning methods. However, the disorder or doping randomness as a tuning parameter creates special difficulties. After all, disorder can fundamentally disturb the basic properties of the material to be tuned. This is particularly true for strongly correlated electron systems. Examples of such are crystal and band-structure changes, the formation of inhomogeneous and non-random clusters, unwelcome magnetic behavior, a metal-to-insulator transition, etc. Hence disorder tuning is a delicate procedure and must be carefully controlled via metallurgical and chemical analyses. Although disorder can create non-Fermi liquid

behavior, the latter can be taken incorrectly as an indication of a QCP. The prime example here is the $Y_{1-x}U_xPd_3$ pseudo-binary alloy, an original non-Fermi liquid without a well-defined ground-state or a QPT (Seaman et al., 1991). Furthermore, magnetic disorder can give rise to a low-temperature spin-glass phase (Mydosh, 2015). This can easily mask the putative QPT by smearing out the QCP into a region of glassy dynamics.

Such effects then pose the question of a percolation transition (Stauffer and Aharony, 1994) caused by lattice or magnetic disorder creating a QPT. Percolation occurs intrinsically from massive disorder and randomness. At the critical percolation concentration a phase transition occurs at zero temperature, does this percolation transition represent a QPT and is the critical concentration a QCP? At the present stage of experimental investigation the percolation behavior does not clearly correspond to a QPT, e.g., the case of $Pd_{1-x}Ni_x$ (Kalvius et al., 2014). And such a result illustrates the stringent challenge of doping disorder as a tuning parameter for a QPT.

The theoretical situation, on the other hand, is at present confused, even for 'clean' transitions tuned by magnetic field or pressure. Sure, there exists the Hertz-Millis theory of itinerant electrons that provides satisfactory answers for a large group of materials, such as $CeNi_2Ge_2$. However, many compounds display clear characteristics that deviate from HM theory, for which only phenomenological theories can currently provide insights. Microscopically, a fundamental unanswered question is the Kondo lattice problem, as well as the theory of quantum critical fluctuations interacting where the electrons cannot be integrated out. Answers to those purely theoretical questions are needed before one can even start to understand specific materials. Luckily, this makes the field of quantum criticality in heavy fermion materials one of the most active and entertaining areas of condensed matter physics.

Acknowledgments

We gratefully acknowledge discussions with Elihu Abrahams, Piers Coleman, Philipp Gegenwart, Hilbert von Löhneysen and Rina Takashima. This work has been supported through an NWO Rubicon fellowship (LR).

References

Abanov, A. and Chubukov, A. V. *Spin-fermion model near the quantum critical point: One-loop renormalization group results.* Phys. Rev. Lett. **84**, 5608–5611, 2000.

Abanov, A. and Chubukov, A. V. *Anomalous Scaling at the Quantum Critical Point in Itinerant Antiferromagnets.* Phys. Rev. Lett. **93**, 255702–4, 2004.

Abrahams, E. and Wölfle, P. *Critical quasiparticle theory applied to heavy fermion metals near an antiferromagnetic quantum phase transition.* Proc. Natl. Acad. Sci. **109**, 3238–3242, 2012.

Abrahams, E., Schmalian, J., and Wölfle, P. *Strong-coupling theory of heavy-fermion criticality.* Phys. Rev. B **90**, 045105–9, 2014.

Amasha, S., Keller, A., Rau, I., Carmi, A., Katine, J., Shtrikman, H., Oreg, Y., and Goldhaber-Gordon, D. *Pseudospin-resolved transport spectroscopy of the Kondo effect in a double quantum dot.* Phys. Rev. Lett. **110**, 046604, 2013.

Ancona-Torres, C., Silevitch, D., Aeppli, G., and Rosenbaum, T. *Quantum and classical glass transitions in $LiHo_xY_{1-x}F_4$.* Phys. Rev. Lett. **101**, 057201, 2008.

Anderson, P. W. *A poor man's derivation of scaling laws for the Kondo problem.* J. Phys. C: Sol. State Phys. **3**, 2436–2441, 1970.

Balents, L. *Spin liquids in frustrated magnets.* Nature **464**, 199–208, 2010.

Bao, W., Pagliuso, P., Sarrao, J., Thompson, J., Fisk, Z., Lynn, J., and Erwin, R. *Incommensurate magnetic structure of $CeRhIn_5$.* Phys. Rev. B **62**, R14621, 2000.

Bianchi, A., Movshovich, R., Vekhter, I., Pagliuso, P., and Sarrao, J. *Avoided Antiferromagnetic Order and Quantum Critical Point in $CeCoIn_5$.* Phys. Rev. Lett. **91**, 257001, 2003.

Bitko, D., Rosenbaum, T., and Aeppli, G. *Quantum critical behavior for a model magnet.* Phys. Rev. Lett. **77**, 940, 1996.

Bloch, I., Dalibard, J., and Zwerger, W. *Many-body physics with ultracold gases.* Rev. Mod. Phys. **80**, 885, 2008.

Bourdarot, F., Martin, N., Raymond, S., Regnault, L.-P., Aoki, D., Taufour, V., and Flouquet, J. *Magnetic properties of URu_2Si_2 under uniaxial stress by neutron scattering.* Phys. Rev. B **84**, 184430, 2011.

Broun, D. *What lies beneath the dome?* Nat. Phys. **4**, 170–172, 2008.

Burdin, S., Georges, A., and Grempel, D. R. *Coherence scale of the Kondo lattice.* Phys. Rev. Lett. **85**, 1048–1051, 2000.

Coldea, R., Tennant, D. A., Wheeler, E. M., and Wawrzynska, E. *Quantum criticality in an Ising chain: experimental evidence for emergent E8 symmetry.* Science , 2010.

Coleman, P. *Theories of non-Fermi liquid behavior in heavy fermions.* Physica B-Condensed Matter **259-61**, 353–358, 1999.

Coleman, P. *Condensed-matter physics - Magnetic spins that last for ever.* Nature **413**, 788–789, 2001.

Coleman, P., Pepin, C., Si, Q., and Ramazashvili, R. *How do Fermi liquids get heavy and die?* J. Phys.-Cond. Mat. **13**, R723–R738, 2001.

Coleman, P. *Heavy Fermions and the Kondo Lattice: a 21st Century Perspective.* arXiv.org, 1509.05769 , 2015.

Coleman, P. and Schofield, A. J. *Quantum criticality.* Nature **433**, 226–229, 2005.

Custers, J., Gegenwart, P., Wilhelm, H., Neumaier, K., Tokiwa, Y., Trovarelli, O., Geibel, C., Steglich, F., Pépin, C., and Coleman, P. *The break-up of heavy electrons at a quantum critical point.* Nature **424**, 524–527, 2003.

Dobrosavljevic, V., Trivedi, N., and Valles Jr, J. M. *Conductor Insulator Quantum Phase Transitions.* Oxford University Press, 2012.

Domb, C. and Lebowitz, J. L. *Phase transitions and critical phenomena.* Academic Press, 2001.

Doniach, S. *The Kondo lattice and weak antiferromagnetism.* Physica B & C **91**, 231–234, 1977.

Fazio, R. and Van Der Zant, H. *Quantum phase transitions and vortex dynamics in superconducting networks.* Phys. Rep. **355**, 235–334, 2001.

Gegenwart, P., Kromer, F., Lang, M., Sparn, G., and Geibel, C. *Non-Fermi-Liquid Effects at Ambient Pressure in a Stoichiometric Heavy-Fermion Compound with Very Low Disorder: $CeNi_2Ge_2$.* Phys. Rev. **82**, 1293–1296, 1999.

Gegenwart, P., Si, Q., and Steglich, F. *Quantum criticality in heavy-fermion metals.* Nat. Phys. **4**, 186–197, 2008.

Georges, A., Kotliar, G., Krauth, W., and Rozenberg, M. J. *Dynamical mean-field theory of strongly correlated fermion systems and the limit of infinite dimensions.* Rev. Mod. Phys. **68**, 13–125, 1996.

Giamarchi, T. *Quantum Phase Transitions in Quasi-One-Dimensional Systems.* In Carr, L. D., editor, *Understanding Quantum Phase Transitions*, chapter 12. CRC Press / Taylor&Francis, 2010.

Giamarchi, T. *Quantum physics in one dimension.* Clarendon Press, 2004.

Goldenfeld, N. *Lectures on phase transitions and the renormalization group.* Addison-Wesley, Advanced Book Program, Reading, 1992.

Greiner, M., Mandel, O., Esslinger, T., Hänsch, T. W., and Bloch, I. *Quantum phase transition from a superfluid to a Mott insulator in a gas of ultracold atoms.* Nature **415**, 39–44, 2002.

Grosche, F. M., Agarwal, P., Julian, S. R., Wilson, N. J., Haselwimmer, R. K. W., Lister, S. J. S., Mathur, N. D., Carter, F. V., Saxena, S. S., and Lonzarich, G. G. *Anomalous low temperature states in $CeNi_2Ge_2$ and $CePd_2Si_2$.* J. Phys.-Cond. Mat. **12**, L533–L540, 2000.

Grosche, F. M. *Quantum phase transitions: Magnetic islands.* Nat. Phys. **10**, 94–95, 2014.

Han, Z., Allain, A., Arjmandi-Tash, H., Tikhonov, K., Feigel'Man, M., Sacépé, B., and Bouchiat, V. *Collapse of superconductivity in a hybrid tin-graphene Josephson junction array.* Nat. Phys. **10**, 380–386, 2014.

Harrison, N., Jaime, M., and Mydosh, J. *Reentrant hidden order at a metamagnetic quantum critical end point.* Phys. Rev. Lett. **90**, 096402, 2003.

Hartmann, S., Oeschler, N., Krellner, C., Geibel, C., Paschen, S., and Steglich, F. *Thermopower evidence for an abrupt Fermi surface change at the quantum critical point of $YbRh_2Si_2$.* Phys. Rev. Lett. **104**, 096401, 2010.

Hassinger, E., Knebel, G., Matsuda, T., Aoki, D., Taufour, V., and Flouquet, J. *Similarity of the Fermi surface in the hidden order state and in the antiferromagnetic state of URu_2Si_2.* Phys. Rev. Lett. **105**, 216409, 2010.

Hegger, H., Petrovic, C., Moshopoulou, E., Hundley, M., Sarrao, J., Fisk, Z., and Thompson, J. *Pressure-induced superconductivity in quasi-2D $CeRhIn_5$.* Phys. Rev. Lett. **84**, 4986, 2000.

Herbut, I. *A Modern Approach to Critical Phenomena.* Cambridge University Press, 2010.

Hertz, J. A. *Quantum Critical Phenomena.* Phys. Rev. B **14**, 1165–1184, 1976.

Heuser, K., Scheidt, E.-W., Schreiner, T., and Stewart, G. *Inducement of non-Fermi-liquid behavior with a magnetic field.* Phys. Rev. B **57**, R4198, 1998.

Hewson, A. C. *The Kondo Problem to Heavy Fermions.* Cambridge University Press, 1993.

Hlubina, R. and Rice, T. M. *Resistivity as a Function of Temperature for Models with Hot-Spots on the Fermi-Surface.* Phys. Rev. B **51**, 9253–9260, 1995.

Jiao, L., Chen, Y., Kohama, Y., Graf, D., Bauer, E., Singleton, J., Zhu, J.-X., Weng, Z., Pang, G., Shang, T., et al. *Fermi surface reconstruction and multiple quantum phase transitions in the antiferromagnet $CeRhIn_5$.* Proc. Natl. Acad. Sci. **112**, 673–678, 2015.

Jönsson, P., Mathieu, R., Wernsdorfer, W., Tkachuk, A., and Barbara, B. *Absence of conventional spin-glass transition in the Ising dipolar system $LiHo_xY_{1-x}F_4$.* Phys. Rev. Lett. **98**, 256403, 2007.

Kalvius, G., Hartmann, O., Wäppling, R., Günther, A., Krimmel, A., Loidl, A., MacLaughlin, D., Bernal, O., Nieuwenhuys, G., Aronson, M., et al. *Magnetism of $Pd_{1-x}Ni_x$ alloys near the critical concentration for ferromagnetism.* Phys. Rev. B **89**, 064418, 2014.

Kambe, S., Sakai, H., Tokunaga, Y., Lapertot, G., Matsuda, T., Knebel, G., Flouquet, J., and Walstedt, R. *Degenerate Fermi and non-Fermi liquids near a quantum critical phase transition.* Nat. Phys. **10**, 840–844, 2014.

Kasuya, T. *A theory of metallic ferro-and antiferromagnetism on Zener's model.* Prog. Theor. Phys. , 1956.

Keimer, B., Kivelson, S., Norman, M., Uchida, S., and Zaanen, J. *From quantum matter to high-temperature superconductivity in copper oxides.* Nature **518**, 179–186, 2015.

Knafo, W. Private communications, 2015.

Knebel, G., Aoki, D., Braithwaite, D., Salce, B., and Flouquet, J. *Coexistence of antiferromagnetism and superconductivity in $CeRhIn_5$ under high pressure and magnetic field.* Phys. Rev. B **74**, 020501, 2006.

Kondo, J. *Resistance Minimum in Dilute Magnetic Alloys.* Prog. Theor. Phys. **32**, 37–49, 1964.

Kopeć, T. *Nonlinear response in quantum spin glasses.* Phys. Rev. Lett. **79**, 4266, 1997.

Kornblit, A. and Ahlers, G. *Heat capacity of EuO near the Curie temperature.* Phys. Rev. B **11**, 2678–2688, 1975.

Küchler, R., Oeschler, N., Gegenwart, P., Cichorek, T., Neumaier, K., Tegus, O., Geibel, C., Mydosh, J. A., Steglich, F., Zhu, L., and Si, Q. *Divergence of the Grüneisen Ratio at Quantum Critical Points in Heavy Fermion Metals.* Phys. Rev. Lett. **91**, 066405–4, 2003.

Küchler, R., Gegenwart, P., Heuser, K., Scheidt, E. W., Stewart, G. R., and Steglich, F. *Grüneisen Ratio Divergence at the*

Quantum Critical Point in $CeCu_{6-x}Ag_x$. Phys. Rev. Lett. **93**, 096402, 2004.

Kummer, K., Patil, S., Chikina, A., Güttler, M., Höppner, M., Generalov, A., Danzenbächer, S., Seiro, S., Hannaske, A., Krellner, C., Kucherenko, Y., Shi, M., Radovic, M., Rienks, E., Zwicknagl, G., Matho, K., Allen, J. W., Laubschat, C., Geibel, C., and Vyalikh, D. V. *Temperature-Independent Fermi Surface in the Kondo Lattice $YbRh_2Si_2$.* Phys. Rev. X **5**, 011028–9, 2015.

Kung, H.-H., Baumbach, R., Bauer, E., Thorsmølle, V., Zhang, W.-L., Haule, K., Mydosh, J., and Blumberg, G. *Chirality density wave of the ?hidden order? phase in URu_2Si_2.* Science **347**, 1339–1342, 2015.

Kuwahara, K., Yoshii, S., Nojiri, H., Aoki, D., Knafo, W., Duc, F., Fabrèges, X., Scheerer, G., Frings, P., Rikken, G., et al. *Magnetic structure of phase II in $U(Ru_{0.96}Rh_{0.04})_2Si_2$ determined by neutron diffraction under pulsed high magnetic fields.* Phys. Rev. Lett. **110**, 216406, 2013.

Lee, S.-S. *Low-energy effective theory of Fermi surface coupled with U(1) gauge field in 2+1dimensions.* Phys. Rev. B **80**, 165102–13, 2009.

Lee, S., Kaul, R. K., and Balents, L. *Interplay of quantum criticality and geometric frustration in columbite.* Nat. Phys. **6**, 702–706, 2010.

Lester, C., Ramos, S., Perry, R., Croft, T., Bewley, R., Guidi, T., Manuel, P., Khalyavin, D., Forgan, E., and Hayden, S. *Field-tunable spin-density-wave phases in $Sr_3Ru_2O_7$.* Nat. Mater. , 2015.

Ma, S.-K. *Modern theory of critical phenomena.* Benjamin, 1976.

Mathur, N. D., Grosche, F. M., Julian, S. R., and Walker, I. R. *Magnetically mediated superconductivity in heavy fermion compounds.* Nature **394**, 39–43, 1998.

Mennenga, G., de Jongh, L., and Huiskamp, W. *Field dependent specific heat study of the dipolar Ising ferromagnet $LiHoF_4$.* J. Magn. Magn. Mater. **44**, 59–76, 1984.

Metlitski, M. A. and Sachdev, S. *Quantum phase transitions of metals in two spatial dimensions. II. Spin density wave order.* Phys. Rev. B **82**, 2010.

Metlitski, M. A., Mross, D. F., Sachdev, S., and Senthil, T. *Cooper pairing in non-Fermi liquids.* Phys. Rev. B **91**, 115111–18, 2015.

Mikeska, H. and Kolezhuk, A. *One-dimensional magnetism.* In Schollwöck, U., Richter, J., Farnell, D. J., and Bishop, R. F., editors, *Quantum Magnetism*, chapter 14. Springer, 2004.

Millis, A. J. *Effect of a Nonzero Temperature on Quantum Critical-Points in Itinerant Fermion Systems.* Phys. Rev. B **48**, 7183–7196, 1993.

Miyake, K., Schmitt-Rink, S., and Varma, C. M. *Spin-Fluctuation-Mediated Even-Parity Pairing in Heavy-Fermion Superconductors.* Phys. Rev. B **34**, 6554–6556, 1986.

Moriya, T. and Takimoto, T. *Anomalous Properties Around Magnetic Instability in Heavy-Electron Systems.* J. Phys. Soc. Jpn. **64**, 960–969, 1995.

Moriya, T. *Spin Fluctuations in Itinerant Electron Magnetism.* Springer-Verlag, Berlin, 1985.

Movshovich, R., Jaime, M., Thompson, J., Petrovic, C., Fisk, Z., Pagliuso, P., and Sarrao, J. *Unconventional Superconductivity in $CeIrIn_5$ and $CeCoIn_5$: Specific Heat and Thermal Conductivity Studies.* Phys. Rev. Lett. **86**, 5152, 2001.

Mydosh, J. *Spin glasses: redux: an updated experimental/materials survey.* Rep. Prog. Phys. **78**, 052501, 2015.

Mydosh, J. and Oppeneer, P. M. *Colloquium: Hidden order, superconductivity, and magnetism: The unsolved case of URu_2Si_2.* Rev. Mod. Phys. **83**, 1301, 2011.

Mydosh, J. A. and Oppeneer, P. M. *Hidden order behaviour in URu_2Si_2 (A critical review of the status of hidden order in 2014).* Philosophical Magazine **94**, 3642–3662, 2014.

Nishimori, H. and Ortiz, G. *Elements of phase transitions and critical phenomena.* OUP Oxford, 2010.

Oeschler, N., Hartmann, S., Pikul, A., Krellner, C., Geibel, C., and Steglich, F. *Low-temperature specific heat of $YbRh_2Si_2$.* Physica B: Cond. Matt. **403**, 1254–1256, 2008.

Oshikawa, M. *Topological approach to Luttinger's theorem and the Fermi surface of a Kondo lattice.* Phys. Rev. Lett. **84**, 3370–3373, 2000.

Paglione, J., Tanatar, M., Hawthorn, D., Boaknin, E., Hill, R., Ronning, F., Sutherland, M., Taillefer, L., Petrovic, C., and Canfield, P. *Field-Induced Quantum Critical Point in $CeCoIn_5$.* Phys. Rev. Lett. **91**, 246405, 2003.

Pankov, S., Florens, S., Georges, A., Kotliar, G., and Sachdev, S. *Non-Fermi-liquid behavior from two-dimensional antiferromagnetic fluctuations: A renormalization-group and large- Nanalysis.* Phys. Rev. B **69**, 054426–12, 2004.

Park, T., Ronning, F., Yuan, H., Salamon, M., Movshovich, R., Sarrao, J., and Thompson, J. *Hidden magnetism and quantum criticality in the heavy fermion superconductor $CeRhIn_5$.* Nature **440**, 65–68, 2006.

Paschen, S., Friedemann, S., Wirth, S., Steglich, F., Kirchner, S., and Si, Q. *Kondo Destruction in Heavy Fermion Quantum Criticality and the Photoemission Spectrum of $YbRh_2Si_2$.* arXiv.org, cond-mat/1507.06088v1 , 2015.

Paschen, S., Lühmann, T., Wirth, S., Gegenwart, P., Trovarelli, O., Geibel, C., Steglich, F., Coleman, P., and Si, Q. *Hall-effect evolution across a heavy-fermion quantum critical point.* Nature **432**, 881–885, 2004.

Petrovic, C., Movshovich, R., Jaime, M., Pagliuso, P., Hundley, M., Sarrao, J., Fisk, Z., and Thompson, J. *A new heavy-fermion superconductor $CeIrIn_5$: A relative of the cuprates?* EPL (Europhysics Letters) **53**, 354, 2001a.

Petrovic, C., Pagliuso, P., Hundley, M., Movshovich, R., Sarrao, J., Thompson, J., Fisk, Z., et al. *Heavy-fermion superconductivity in $CeCoIn_5$ at 2.3 K.* J. Phys.: Cond. Mat. **13**, L337, 2001b.

Pfleiderer, C., Mydosh, J., and Vojta, M. *Pressure dependence of the magnetization of URu_2Si_2.* Phys. Rev. B **74**, 104412, 2006.

Pfleiderer, C. *Superconducting phases of f-electron compounds.* Rev. Mod. Phys. **81**, 1551–1624, 2009.

Pham, L., Park, T., Maquilon, S., Thompson, J., and Fisk, Z. *Reversible tuning of the heavy-fermion ground state in $CeCoIn_5$.*

Phys. Rev. Lett. **97**, 056404, 2006.

Quilliam, J., Meng, S., Kycia, J., et al. *Experimental phase diagram and dynamics of a dilute dipolar-coupled Ising system.* Phys. Rev. B **85**, 184415, 2012.

Rau, I., Amasha, S., Oreg, Y., and Goldhaber-Gordon, D. *Quantum Phase Transitions in Quantum Dots.* In Carr, L. D., editor, *Understanding Quantum Phase Transitions*, chapter 12. CRC Press / Taylor&Francis, 2010.

Read, N., Sachdev, S., and Ye, J. *Landau theory of quantum spin glasses of rotors and Ising spins.* Phys. Rev. B **52**, 384, 1995.

Reich, D., Rosenbaum, T., Aeppli, G., and Guggenheim, H. *Ferromagnetism, glassiness, and metastability in a dilute dipolar-coupled magnet.* Phys. Rev. B **34**, 4956, 1986.

Rodriguez, J., Aczel, A. A., Carlo, J., Dunsiger, S., Macdougall, G. J., Russo, P. L., Savici, A. T., Uemura, Y. J., Wiebe, C., and Luke, G. M. *Study of the Ground State Properties of $LiHo_xY_{1-x}F_4$ Using Muon Spin Relaxation.* Phys. Rev. Lett. **105**, 107203, 2010.

Rønnow, H., Parthasarathy, R., Jensen, J., Aeppli, G., Rosenbaum, T., and McMorrow, D. *Quantum phase transition of a magnet in a spin bath.* Science **308**, 389–392, 2005.

Rønnow, H., Jensen, J., Parthasarathy, R., Aeppli, G., Rosenbaum, T., McMorrow, D., and Kraemer, C. *Magnetic excitations near the quantum phase transition in the Ising ferromagnet $LiHoF_4$.* Phys. Rev. B **75**, 054426, 2007.

Rosch, A. *Interplay of disorder and spin fluctuations in the resistivity near a quantum critical point.* Phys. Rev. Lett. **82**, 4280–4283, 1999.

Rosch, A. *Magnetotransport in nearly antiferromagnetic metals.* Phys. Rev. B **62**, 4945–4962, 2000.

Rosch, A., Schroder, A., Stockert, O., and von Löhneysen, H. *Mechanism for the non-Fermi-liquid behavior in $CeCu_{6-x}Au_x$.* Phys. Rev. Lett. **79**, 159–162, 1997.

Rowley, S., Spalek, L., Smith, R., Dean, M., Itoh, M., Scott, J., Lonzarich, G., and Saxena, S. *Ferroelectric quantum criticality.* Nat. Phys. **10**, 367–372, 2014.

Ruderman, M. A. and Kittel, C. *Indirect exchange coupling of nuclear magnetic moments by conduction electrons.* Phys. Rev. **96**, 99–102, 1954.

Sachdev, S. *Colloquium: Order and quantum phase transitions in the cuprate superconductors.* Rev. Mod. Phys. **75**, 913, 2003.

Sachdev, S. *Quantum magnetism and criticality.* Nat. Phys. **4**, 173–185, 2008.

Sachdev, S. *Quantum Phase Transitions.* Cambridge University Press, 2011.

Scalapino, D. J., Loh Jr, E., and Hirsch, J. E. *d-wave pairing near a spin-density-wave instability.* Phys. Rev. B **34**, 8190–8192, 1986.

Schechter, M. *$LiHo_xY_{1-x}F_4$ as a random-field Ising ferromagnet.* Phys. Rev. B **77**, 020401, 2008.

Schröder, A., Lynn, J., Erwin, R., Loewenhaupt, M., and von Löhneysen, H. *Magnetic structure of the heavy fermion alloy $CeCu_{5.5}Au_{0.5}$.* Physica B: Cond. Matt. **199**, 47–48, 1994.

Schröder, A., Aeppli, G., Coldea, R., Adams, M., Stockert, O., von Löhneysen, H., Bucher, E., Ramazashvili, R., and Coleman, P. *Onset of antiferromagnetism in heavy-fermion metals.* Nature **407**, 351–355, 2000.

Seaman, C., Maple, M., Lee, B., Ghamaty, S., Torikachvili, M., Kang, J.-S., Liu, L., Allen, J., and Cox, D. *Evidence for non-Fermi liquid behavior in the Kondo alloy $Y_{1-x}U_xPd_3$.* Phys. Rev. Lett. **67**, 2882, 1991.

Sengupta, A. M. *Spin in a fluctuating field: the Bose (+ Fermi) Kondo models.* Phys. Rev. B **61**, 4041–4043, 2000.

Senthil, T. *Critical Fermi surfaces and non-Fermi liquid metals.* Phys. Rev. B **78**, 035103–14, 2008.

Senthil, T., Sachdev, S., and Vojta, M. *Fractionalized Fermi Liquids.* Phys. Rev. Lett. **90**, 216403–4, 2003.

Senthil, T., Vojta, M., and Sachdev, S. *Weak magnetism and non-Fermi liquids near heavy-fermion critical points.* Phys. Rev. B **69**, 035111–19, 2004.

Seo, S., Lu, X., Zhu, J., Urbano, R., Curro, N., Bauer, E., Sidorov, V., Pham, L., Park, T., Fisk, Z., et al. *Disorder in quantum critical superconductors.* Nat. Phys. **10**, 120–125, 2014.

Shang, T., Baumbach, R., Gofryk, K., Ronning, F., Weng, Z., Zhang, J., Lu, X., Bauer, E., Thompson, J., and Yuan, H. *$CeIrIn_5$: Superconductivity on a magnetic instability.* Phys. Rev. B **89**, 041101, 2014.

She, J.-H. and Zaanen, J. *BCS superconductivity in quantum critical metals.* Phys. Rev. B **80**, 184518–15, 2009.

Shibauchi, T., Carrington, A., and Matsuda, Y. *A Quantum Critical Point Lying Beneath the Superconducting Dome in Iron Pnictides.* Annual Review of Condensed Matter Physics **5**, 113–135, 2014.

Shishido, H., Settai, R., Harima, H., and Ōnuki, Y. *A drastic change of the Fermi surface at a critical pressure in $CeRhIn_5$: dHvA study under pressure.* J. Phys. Soc. Jpn. **74**, 1103–1106, 2005.

Si, Q. and Steglich, F. *Heavy fermions and quantum phase transitions.* Science **329**, 1161–1166, 2010.

Si, Q., Rabello, S., Ingersent, K., and Smith, J. L. *Locally critical quantum phase transitions in strongly correlated metals.* Nature **413**, 804–808, 2001.

Si, Q., Pixley, J. H., Nica, E., Yamamoto, S. J., Goswami, P., Yu, R., and Kirchner, S. *Kondo Destruction and Quantum Criticality in Kondo Lattice Systems.* J. Phys. Soc. Jpn. **83**, 061005–11, 2014.

Sidorov, V., Nicklas, M., Pagliuso, P., Sarrao, J., Bang, Y., Balatsky, A., and Thompson, J. *Superconductivity and Quantum Criticality in $CeCoIn_5$.* Phys. Rev. Lett. **89**, 157004, 2002.

Stanley, H. E. *Introduction to phase transitions and critical phenomena.* Oxford University Press, 1971.

Stauffer, D. and Aharony, A. *Introduction to percolation theory.* CRC press, 1994.

Steppke, A., Küchler, R., Lausberg, S., Lengyel, E., Steinke, L., Borth, R., Lühmann, T., Krellner, C., Nicklas, M., Geibel, C., Steglich, F., and Brando, M. *Ferromagnetic Quantum Critical Point in the Heavy-Fermion Metal $YbNi_4(P_{1-x}As_x)_2$.* Science **339**, 933–936, 2013.

Stewart, G. *Non-Fermi-liquid behavior in d-and f-electron metals.* Rev. Mod. Phys. **73**, 797, 2001.

Stewart, G. *Addendum: Non-Fermi-liquid behavior in d-and f-electron metals.* Rev. Mod. Phys. **78**, 743, 2006.

Stock, C., Broholm, C., Demmel, F., Van Duijn, J., Taylor, J., Kang, H., Hu, R., and Petrovic, C. *From incommensurate correlations to mesoscopic spin resonance in $YbRh_2Si_2$.* Phys. Rev. Lett. **109**, 127201, 2012.

Stockert, O., von Löhneysen, H., Rosch, A., Pyka, N., and Loewenhaupt, M. *Two-dimensional fluctuations at the quantum-critical point of $CeCu_{6-x}Au_x$.* Phys. Rev. Lett. **80**, 5627, 1998.

Stockert, O., Faulhaber, E., Zwicknagl, G., Stüßer, N., Jeevan, H. S., Deppe, M., Borth, R., Küchler, R., Loewenhaupt, M., Geibel, C., and Steglich, F. *Nature of the APhase in $CeCu_2Si_2$.* Phys. Rev. Lett. **92**, 136401–4, 2004.

Stockert, O., Kirchner, S., Steglich, F., and Si, Q. *Superconductivity in Ce-and U-Based '122' Heavy-Fermion Compounds.* J. Phys. Soc. Jpn. **81**, 011001, 2011.

Suzuki, M. *Relationship Between D-Dimensional Quantal Spin Systems and (D+1)-Dimensional Ising Systems - Equivalence, Critical Exponents and Systematic Approximants of Partition-Function and Spin Correlations.* Prog. Theor. Phys. **56**, 1454–1469, 1976.

Tabei, S., Gingras, M., Kao, Y.-J., Stasiak, P., and Fortin, J.-Y. *Induced Random Fields in the $LiHo_xY_{1-x}F_4$ Quantum Ising Magnet in a Transverse Magnetic Field.* Phys. Rev. Lett. **97**, 237203, 2006.

Tokiwa, Y., Radu, T., Geibel, C., Steglich, F., and Gegenwart, P. *Divergence of the Magnetic Grüneisen Ratio at the Field-Induced Quantum Critical Point in $YbRh_2Si_2$.* Phys. Rev. Lett. **102**, 066401–4, 2009.

Tokiwa, Y., Ishikawa, J., Nakatsuji, S., and Gegenwart, P. *Quantum criticality in a metallic spin liquid.* Nat. Mater. **13**, 356–359, 2014.

Trovarelli, O., Geibel, C., Mederle, S., Langhammer, C., Grosche, F., Gegenwart, P., Lang, M., Sparn, G., and Steglich, F. *$YbRh_2Si_2$: Pronounced non-Fermi-liquid effects above a low-lying magnetic phase transition.* Phys. Rev. Lett. **85**, 626, 2000.

Urbano, R., Young, B.-L., Curro, N., Thompson, J., Pham, L., and Fisk, Z. *Interacting antiferromagnetic droplets in quantum critical $CeCoIn_5$.* Phys. Rev. Lett. **99**, 146402, 2007.

Valla, T., Fedorov, A., Johnson, P., Wells, B., Hulbert, S., Li, Q., Gu, G., and Koshizuka, N. *Evidence for quantum critical behavior in the optimally doped cuprate $Bi_2Sr_2CaCu_2O_{8+\delta}$.* Science **285**, 2110–2113, 1999.

Vandervelde, D., Yuan, H., Onuki, Y., and Salamon, M. *Evidence of d-wave pairing symmetry of the gap of the heavy-fermion superconductor $CeIrIn_5$ from magnetic-penetration-depth measurements.* Phys. Rev. B **79**, 212505, 2009.

Varma, C. *Quantum Criticality in Quasi-Two Dimensional Itinerant Antiferromagnets.* Phys. Rev. Lett. **115**, 186405, 2015.

Villaume, A., Bourdarot, F., Hassinger, E., Raymond, S., Taufour, V., Aoki, D., and Flouquet, J. *SigNature of hidden order in heavy fermion superconductor URu_2Si_2: Resonance at the wave vector $Q_0 = (1, 0, 0)$.* Phys. Rev. B **78**, 012504, 2008.

Vojta, M., Bulla, R., and Wölfle, P. *Critical quasiparticles in single-impurity and lattice Kondo models.* arXiv.org, 1507.04595 , 4595–1146, 2015.

von Löhneysen, H., Pietrus, T., Portisch, G., Schlager, H., Schröder, A., Sieck, M., and Trappmann, T. *Non-Fermi-liquid behavior in a heavy-fermion alloy at a magnetic instability.* Phys. Rev. Lett. **72**, 3262, 1994.

von Löhneysen, H., Pfleiderer, C., Pietrus, T., Stockert, O., and Will, B. *Pressure versus magnetic-field tuning of a magnetic quantum phase transition.* Phys. Rev. B **63**, 134411, 2001.

von Löhneysen, H. *Non-fermi-liquid behaviour in the heavy-fermion system.* J. Phys. Cond. Matt. **8**, 9689, 1996.

von Löhneysen, H., Rosch, A., Vojta, M., and Wölfle, P. *Fermi-liquid instabilities at magnetic quantum phase transitions.* Rev. Mod. Phys. **79**, 1015–1075, 2007.

Westerkamp, T., Deppe, M., Küchler, R., Brando, M., Geibel, C., Gegenwart, P., Pikul, A. P., and Steglich, F. *Kondo-Cluster-Glass State near a Ferromagnetic Quantum Phase Transition.* Phys. Rev. Lett. **102**, 206404–4, 2009.

Wilson, K. G. and Kogut, J. *The renormalization group and the ϵ expansion.* Physics Reports **12**, 75–199, 1974.

Wölfle, P. and Abrahams, E. *Quasiparticles beyond the Fermi liquid and heavy fermion criticality.* Phys. Rev. B **84**, 041101–4, 2011.

Wölfle, P. and Abrahams, E. *Spin-flip scattering of critical quasiparticles and the phase diagram of $YbRh_2Si_2$.* arXiv.org, 1506.08476 , 8476, 2015.

Wu, L., Kim, M., Park, K., Tsvelik, A., and Aronson, M. *Quantum critical fluctuations in layered YFe_2Al_{10}.* Proc. Natl. Acad. Sci. **111**, 14088–14093, 2014.

Wu, W., Bitko, D., Rosenbaum, T., and Aeppli, G. *Quenching of the nonlinear susceptibility at a T= 0 spin glass transition.* Phys. Rev. Lett. **71**, 1919, 1993.

Yeomans, J. M. *Statistical Mechanics of Phase Transitions.* Oxford Science Publications, 1992.

Yosida, K. *Magnetic properties of Cu-Mn alloys.* Phys. Rev. **106**, 893–898, 1957.

Zapf, V., Jaime, M., and Batista, C. *Bose-Einstein condensation in quantum magnets.* Rev. Mod. Phys. **86**, 563, 2014.

Zhu, L., Garst, M., Rosch, A., and Si, Q. *Universally Diverging Grüneisen Parameter and the Magnetocaloric Effect Close to Quantum Critical Points.* Phys. Rev. Lett. **91**, 066404–4, 2003.